entry. Thus, timely uncoating was thought to be important for efficient HIV-1 infection. In agreement with this idea, anti-HIV factors TRIM5α and TRIMCyp were shown to bind viral core and accelerate uncoating, thus abrogating productive RT [13–17]. This observation suggests that the core persists as a defined structure for a certain period of time after fusion. Intriguingly, Yamashita et al. showed that CA is important for HIV-1 infection of non-dividing cells [11,18]. In addition, the transportin-SR2 (or TNPO3) -dependence of HIV-1 nuclear entry has been mapped to the HIV-1 CA [19,20]. These results also suggest a functional link between the HIV-1 CA and nuclear entry.

We previously generated simian-tropic HIV-1 that replicates efficiently in cynomolgus monkey (CM) cells [21]. This virus encodes a CA with SIVmac239-derived loops between α-helices 4 and 5 (L4/5) and between α-helices 6 and 7 (L6/7), along with the entire SIVmac239 *vif*. These SIVmac239-derived sequences allow HIV-1 to escape from restriction factors in monkey cells, including cyclophilin A (CypA), TRIM5α, and ApoB mRNA editing catalytic subunit (APOBEC) 3G. However, the replicative capability of this virus (NL-4/5S6/7SvifS) in human cells was severely impaired. By long-term cultivation of human CEM-SS cells infected with NL-4/5S6/7SvifS, we succeeded in partially rescuing the replicative capability of this virus in human cells [22]. This adapted virus encoded a G-to-E substitution at the 116th position of the CA (NL-4/5SG116E6/7SvifS). Interestingly, this G116E mutation also occurred after adaptation in rhesus monkey cells [23].

In the work presented here, we examined the mechanism by which the replicative capability of NL-4/5S6/7SvifS was severely impaired in human cells.

Materials and Methods

Cells

The human kidney adherent 293T cells and the human cervical cancer HeLa cells were cultured in Dulbecco's modified Eagle medium supplemented with 10% heat-inactivated fetal bovine serum (FBS). Cells of the human T cell line CEM-SS were maintained in RPMI 1640 medium supplemented with 10% FBS.

Virus propagation

Virus stocks were prepared by transfection of 293T cells with HIV-1 derivatives described previously [21,22,24] using polyethylenimine (PEI) (molecular weight, 25,000; Polysciences). As shown in Figure 1A, NL-vifS possesses the entire *vif* of SIVmac239 in the background of HIV-1 NL4-3 (NL-SVR in reference [24]). NL-4/5S6/7SvifS encodes CA with the SIVmac239-derived L4/5 and L6/7 in the background of NL-vifS [21]. NL-4/5SG116E6/7SvifS encodes a CA with an additional G-to-E substitution at the 116th position, in the background of NL-4/5S6/7SvifS [22]. NL-Nh is a mutant of the NL4-3 proviral clone in which an *Nhe*I restriction enzyme cleavage site was blunted and re-ligated, introducing frame-shift mutations in the *env* gene [25]. For NL-Nh, GFP-expressing NL4-3-derived HIV-1 proviral clone MSMnG [25], and luciferase-expressing NL4-3-Luc-R-E- (NIH AIDS Research and Reference Reagent Program), the *BssH*II to *Apa*I fragment (corresponding to the majority of the *gag* gene) was replaced with the corresponding fragment of NL-4/5S6/7SvifS or NL-4/5SG116E6/7SvifS. Viral titers were measured with the RETROtek antigen ELISA kit (ZeptoMetrix, Buffalo, NY).

Viral infections

CEM-SS cells (2 x 10^5 per reaction) were infected with HIV-1 derivatives at titers equivalent to 20 ng of p24 per reaction. Culture supernatants were collected periodically, and p24 levels were measured using an ELISA kit.

Real-time PCR analysis

CEM-SS cells (1 x 10^6 per reaction) were infected with DNase I-pretreated HIV-1 derivatives at titers equivalent to 80 ng of p24 per reaction. DNase I pretreatment consisted of incubation with DNase I (20 units/ml in 10 mM $MgCl_2$) for 30 min at room temperature. After 2 hr on ice, infected cells were washed with PBS, resuspended in medium, and returned to 37° C until harvesting at the indicated time point post-infection. Genomic DNA was extracted by using the QIAamp DNA Blood Mini kit (Qiagen). After digestion with 1 unit/μl *Dpn*I for 4 hr at 37° C, 30 ng of DNA was analyzed for U5/gag, 2-LTR, and Alu-HIV by real-time PCR using published primers and TaqMan probes [26,27] in an Applied Biosystems 7500 Real-Time PCR System.

In situ uncoating assay

The *in situ* uncoating assay was conducted as previously described [11,28]. Briefly, the labeled virus was generated by cotransfecting 9 μg NL-Nh CA mutant proviral plasmid, 4 μg S15-dTomato-expressing plasmid, 4 μg vesicular stomatitis virus G protein (VSV-G)-expressing plasmid, and 1 μg GFP-Vpr-expressing plasmid into 10-cm plates of 293T cells using PEI. HeLa cells were spinoculated with the labeled virus for 2 hr at 16° C in the presence or absence of bafilomycin A (BafA) (Sigma). Virus-containing supernatant then was removed and replaced with 37° *C medium* in the presence or absence of BafA, shifted to 37° C, and fixed with 3.7% formaldehyde (Polysciences) in 0.1M PIPES buffer (pH 6.8) at the indicated time point post-infection. The fixed HeLa cells were permeabilized with blocking solution (0.1 M PIPES [pH 6.8], 10% normal donkey serum [Jackson ImmunoResearch Laboratories], 0.01% Triton X-100, 0.01% NaN_3) for 5 min at room temperature, stained with anti-p24 mAb AG3.0 (NIH AIDS Research and Reference Reagent Program) in blocking solution without Triton X-100 for 1 hr at room temperature for primary staining, and secondarily stained with labeled Cy5 donkey anti-mouse antibodies (Jackson ImmunoResearch Laboratories) for 30 min at room temperature. Images were collected and deconvolved with a Deltavision microscope and software (Applied Precision). Following deconvolution, images were blinded for identity to remove bias during counting. The number of GFP-positive virions was assessed at each time point, and each virion was individually inspected for punctate dTomato fluorescent signal and p24 Cy-5 signal.

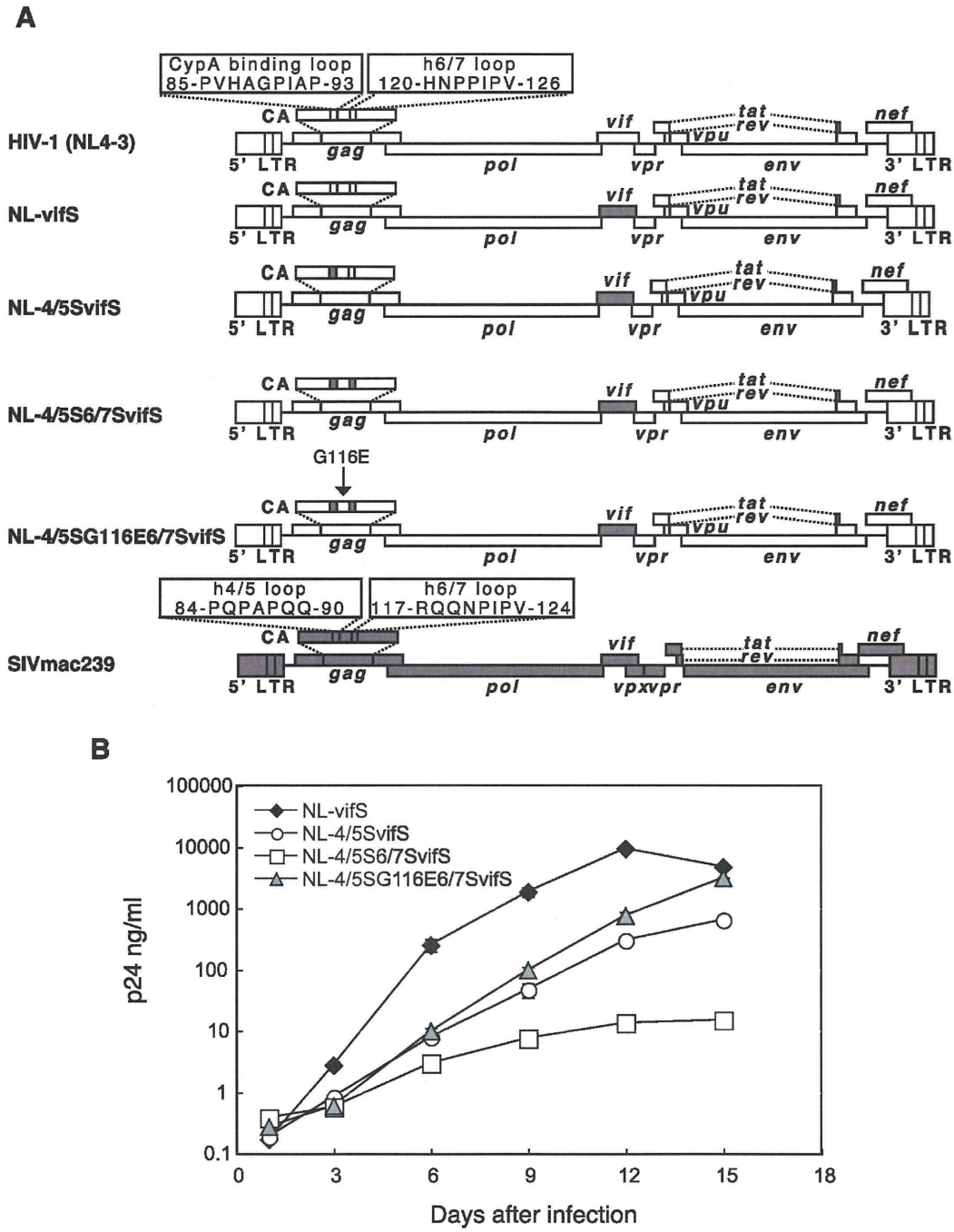

Figure 1. Structure of the simian-tropic HIV-1 clones and the replication properties in human cells. (A) White bars denote HIV-1 (NL4-3) and gray bars SIVmac239 sequences. (B) Equal amounts of NL-vifS (black diamonds), NL-4/5SvifS (white circles), NL-4/5S6/7SvifS (white squares), and NL-4/5SG116E6/7SvifS (gray triangles) were inoculated into human CEM-SS cells, and culture supernatants were collected periodically. p24 antigen levels were measured by ELISA. Error bars reflect actual fluctuations of duplicate infections.

doi: 10.1371/journal.pone.0072531.g001

Statistical analysis

Differences in luciferase activities, amounts of late RT products, and uncoating kinetics were evaluated with unpaired t tests.

Results

The replicative capability of NL-4/5S6/7SvifS was impaired in human cells, while that of NL-4/5SG116E6/7SvifS was partially rescued by a single amino acid mutation in CA

Several HIV-1 derivatives have been constructed to establish a monkey model of HIV-1/AIDS (Figure 1A). NL-4/5SvifS could replicate in CM cells [24]. Introduction into NL-4/5SvifS of SIVmac239 L6/7, which is a determinant of HIV type 2 (HIV-2) CM TRIM5α sensitivity [29], improved viral growth in CM cells [21]. However, the replicative capability of the resultant virus (NL-4/5S6/7SvifS) in human cells was greatly attenuated. After long-term cultivation of human CEM-SS cells infected with NL-4/5S6/7SvifS, we succeeded in partially rescuing the impaired replicative capability of the virus [22]. This adapted virus (NL-4/5SG116E6/7SvifS) encoded a G-to-E substitution at the 116th position of NL4-3 CA sequence. Figure 1B shows the replication of NL-vifS that possesses the entire *vif* of SIVmac in the background of HIV-1, NL-4/5SvifS, NL-4/5S6/7SvifS, and NL-4/5SG116E6/7SvifS in human CEM-SS cells. Consistent with our previous report [22], the replicative capability of NL-4/5S6/7SvifS was severely impaired in human cells (Figure 1B). On the other hand, the replicative capability of NL-4/5SG116E6/7SvifS was improved compared with that of NL-4/5S6/7SvifS, and slightly better than that of NL-4/5SvifS, even though replication did not reach the levels seen with NL-vifS.

We then inoculated CEM-SS cells with VSV-G-pseudotyped luciferase- expressing HIV-1 vector encoding wild type (WT), 4/5S6/7S, or 4/5SG116E6/7S CA. As shown in Figure 2A, infectivity was significantly reduced by the 4/5S6/7S mutation ($p<0.0001$), and infectivity was restored by addition of the G116E mutation to 4/5S6/7S ($p=0.0004$). Similar results were obtained when we used a VSV-G-pseudotyped GFP-expressing version of the HIV-1 vector (Figure 2B). These results clearly indicated that the different replicative capability of the viruses was due mainly to effects at the early stage of viral replication.

Levels of NL-4/5S6/7SvifS RT products were decreased at 12 hours after infection

To determine which step of NL-4/5S6/7SvifS early infection stage was impaired, we first measured RT products of replication-competent viruses NL-vifS, NL-4/5S6/7SvifS, and NL-4/5SG116E6/7SvifS in CEM-SS cells. At 12 hr after infection, the amounts of U5/gag (late RT products) and 2-LTR circles (a surrogate for nuclear entry) of NL-4/5S6/7SvifS were 69.4% ($p=0.0270$) and 38.6% ($p=0.0003$) of those of NL-vifS, respectively (Figure 3A). These results suggested that NL-4/5S6/7SvifS has defects in both RT and nuclear entry. On the other hand, the amount of Alu-HIV (integrated viral DNA) of NL-4/5S6/7SvifS was 38.2% ($p=0.0029$) that of NL-vifS, being

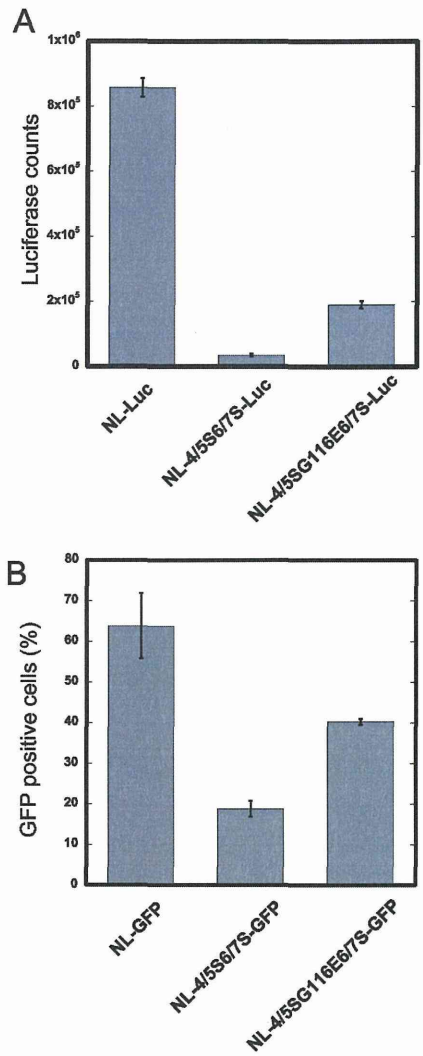

Figure 2. Single round infection assays. (A) 3X10^5 CEM-SS cells were infected with viral titers equivalent to 5 ng of p24 of VSV-G-pseudotyped luciferase-expressing viruses with NL4-3 CA (NL-Luc), 4/5S6/7S CA (NL-4/5S6/7S-Luc), or 4/5SG116E6/7S CA (NL-4/5SG116E6/7S-Luc). The luciferase activity was measured at 48 hr after infection by a luminometer. Error bars reflect the SD of triplicate infections. Presented data are representative of two independent experiments using a different set of molecular clones. (B) 3X10^5 CEM-SS cells were infected with viral titers equivalent to 80 ng of p24 of VSV-G-pseudotyped GFP-expressing viruses with NL4-3 CA (NL-GFP), NL-4/5S6/7S CA (NL-4/5S6/7S-GFP), or NL-4/5SG116E6/7S CA (NL-4/5SG116E6/7S-GFP). The GFP-positive cells were counted at 24 hr after infection by a flow cytometer. Error bars reflect the SD of triplicate infections. Presented data are representative of two independent experiments using a different set of molecular clones.

doi: 10.1371/journal.pone.0072531.g002

comparable to that of 2-LTR circles. These results suggested that NL-4/5S6/7SvifS has WT-like ability to integrate after nuclear entry. In the case of NL-4/5SG116E6/7SvifS, the amount of late RT, 2-LTR, and Alu-HIV were 67.5% (p=0.0216), 38.4% (p=0.0005), and 38.5% (p=0.0052) of NL-vifS, respectively. These results suggested that NL-4/5SG116E6/7SvifS also was impaired for RT and nuclear entry. We failed to detect any significant recovery of late RT (p=0.88), 2-LTR (p=0.98), or Alu-HIV (p=0.98) of NL-4/5SG116E6/7SvifS by addition of the G116E mutation to NL-4/5S6/7SvifS.

We then measured RT products during a 72-hr time course (Figure 3B). The amount of late RT products of NL-4/5S6/7SvifS and NL-4/5SG116E6/7SvifS were decreased to similar extents at 24 hr after infection (Figure 3B upper panel), likely because of degradation of unproductive products. Supporting this idea, the levels of Alu-HIV, an outcome of productive infection, continued to increase in cells infected with these viruses (Figure 3B lower panel). On the other hand, the level of late RT of NL-vifS at 24 hr after infection was almost the same as that at 12 hr after infection. This persistence is likely due to the balance between degradation of unproductive RT products from the first round of infection and newly generated RT products from the second-round infection by the progeny viruses, since this experiment used replication-competent viruses. In the cases of NL-4/5S6/7SvifS and NL-4/5SG116E6/7SvifS, the RT products from the second-round infection also would be impaired. Thus, these viruses were not expected to overcome the degradation of unproductive RT products of the initial infection. The difference of late RT, 2-LTR, and Alu-HIV between NL-4/5S6/7SvifS and NL-4/5SG116E6/7SvifS gradually expanded at 48 and 72 hr after infection, presumably due to the effects of multiple rounds of infection. This result was in good agreement with that of the p24 production shown in Figure 1B.

The levels of late RT product of NL-4/5S6/7SvifS were increased at the earlier time points of infection

To determine the mechanisms of the decreased RT production of NL-4/5S6/7SvifS and NL-4/5SG116E6/7SvifS, we analyzed RT at earlier time points after infection. Contrary to our expectation, the amount of late RT products of NL-4/5S6/7SvifS exceeded that of NL-vifS at 4 and 8 hr after infection (Figure 4A). This result indicated that the kinetics of RT product generation was faster for NL-4/5S6/7SvifS than for NL-vifS, despite the fact that the 12-hr levels of late RT products were lower with NL-4/5S6/7SvifS than with NL-vifS (Figures 3A and 4A). The late RT production of NL-4/5S6/7SvifS peaked at 8 hr after infection before decreasing at 12 hr after infection. In contrast, late RT products of NL-vifS gradually increased until 12 hr after infection. The peak amount of late RT products with NL-4/5S6/7SvifS was comparable to that with NL-vifS. Thus we conclude that NL-4/5S6/7SvifS had a defect not in RT but in nuclear entry, and that the synthesized viral cDNA that failed to enter the nucleus was degraded.

In a sharp contrast to NL-4/5S6/7SvifS, NL-4/5SG116E6/7SvifS yielded reduced amounts of late RT products compared to NL-vifS at the respective time points. Similar to NL-vifS, however, the late RT products of NL-4/5SG116E6/7SvifS gradually increased until 12 hr after infection. These findings also were unexpected and indicated that the single G-to-E substitution (which at least partially rescued the impaired replicative capability of NL-4/5S6/7SvifS in human cells) also attenuated late RT at the earlier time points. Therefore, the mechanism underlying decreased late RT product levels of NL-4/5S6/7SvifS at 12 hr after infection seemed to be totally different from that of NL-4/5SG116E6/7SvifS.

Next, we measured amounts of RT product of aforementioned VSV-G-pseudotyped GFP-expressing HIV-1 vectors in a single-round infection assay to confirm the results seen with replication-competent viruses. The absolute copy numbers of RT products of GFP-expressing viruses were less than those of replication-competent viruses, probably due to increase of genome size by reporter gene insertion. However, amounts of the late RT products of the virus encoding 4/5S6/7S CA at 8 hr after infection exceeded those of the virus encoding NL4-3 CA (p=0.04, Figure 4B), as observed in replication-competent viruses. At 16 hr after infection, the amounts of the late RT products of the virus encoding 4/5S6/7S CA were less than those of the virus encoding NL4-3 CA (p=0.007, Figure 4B), consistent with the results of replication-competent viruses. Furthermore, amounts of late RT products of the virus encoding 4/5S116E6/7S CA were lower than those of the virus encoding NL4-3 CA at 16 hr after infection (p=0.009, Figure 4B). Thus, the results of replication-incompetent viruses clearly confirmed the results of replication-competent viruses. Similar results also were obtained when we used VSV-G-pseudotyped NL-Nh versions of the viruses (data not shown).

The uncoating kinetics of NL-4/5S6/7S was slower than that of the virus with the NL4-3 CA

Several studies have reported that mutations in CA affected viral core stability and resulted in deleterious effects on RT [4] or nuclear entry [12]. To determine whether the CA mutations in NL-4/5S6/7SvifS or NL-4/5SG116E6/7SvifS affect the core stability, we performed an *in situ* uncoating assay according to the method described previously [11,28]. For our experiment, a replication-incompetent virus (NL-Nh), which carries a frame-shift mutation in the *env* gene, was used as the wild type virus. The CA of NL-Nh was replaced with that of NL-4/5S6/7SvifS or NL-4/5SG116E6/7SvifS, since the virus had to be pseudotyped with VSV-G. NL-Nh, NL-Nh mutant encoding 4/5S6/7S CA, and NL-Nh mutant encoding 4/5SG116E6/7S CA were labeled with GFP-Vpr, while the viral membrane was labeled with S15-dTomato; the membrane label was expected to disappear after productive fusion of the virion into the cytoplasm. To provide a negative control reaction, bafilomycin A (BafA) was included to block fusion of the virus and cellular membranes. This control was used to confirm that unfused viral particles fail to undergo uncoating. Infection was synchronized and at various times after infection the cells were fixed and stained with an antibody to p24 CA. The total number of complexes that entered the cytoplasm (green spots that lost S15-dTomato) was counted,

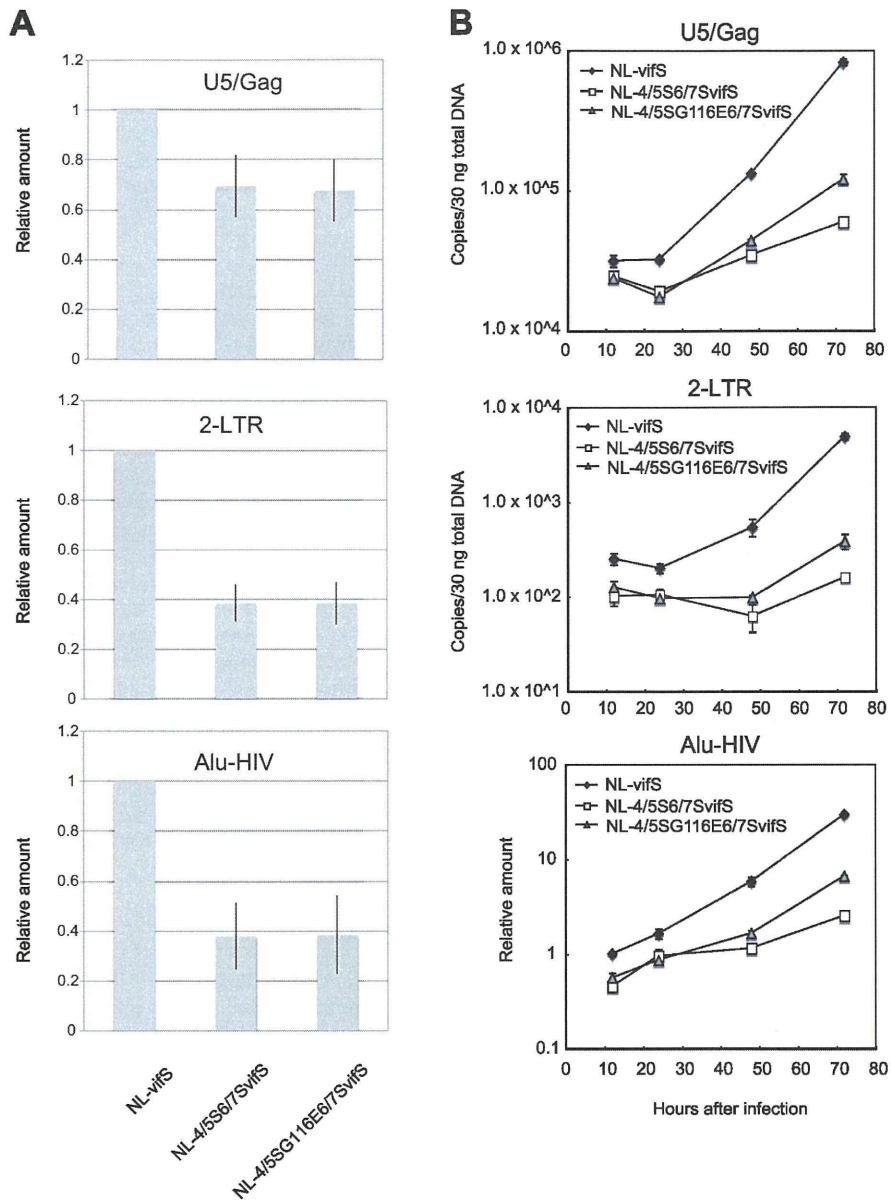

Figure 3. Measurement of the reverse transcribed products of simian-tropic HIV-1 in human cells. (A) CEM-SS cells were infected with NL-vifS, NL-4/5S6/7SvifS, or NL-4/5SG116E6/7SvifS, and DNA was extracted at 12 hr after infection and subjected to real-time PCR assays using U5/gag primers for late reverse transcription (RT), 2-LTR primers for nuclear transported viral DNA, and Alu-HIV primers for integrated DNA. Mean relative amounts of U5/gag, 2-LTR, and Alu-HIV products obtained from three independent experiments (the amount in the NL-vifS sample at 12 hr after infection is set at 1) are indicated. Mean numbers of U5/gag, 2-LTR, and Alu-HIV copies per 30 ng of total DNA of NL-vifS-infected cells were 39695, 187, and 2.17, respectively. Error bars reflect the SD of the three independent experiments. (B) CEM-SS cells were infected with NL-vifS, NL-4/5S6/7SvifS, or NL-4/5SG116E6/7SvifS, and DNA was extracted at 12, 24, 48, and 72 hr after infection and subjected to real-time PCR assays as described above. The number of viral DNA (U5/gag and 2-LTR) copies per 30 ng of total DNA and relative amount of Alu-HIV products (the amount in the NL-vifS sample at 12 hr after infection is set at 1) is indicated. Error bars reflect the SD of triplicate values of real-time PCR. Presented data are representative of three independent experiments.

doi: 10.1371/journal.pone.0072531.g003

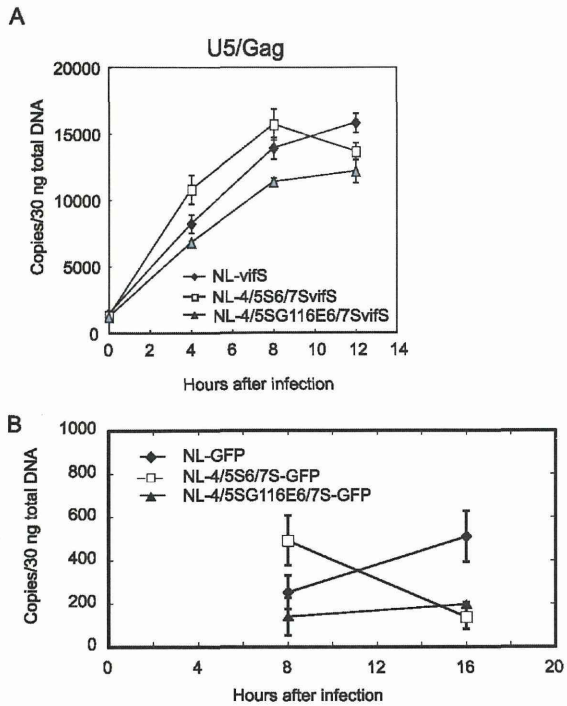

Figure 4. Measurement of the U5/gag (late RT products) during a 12-hr time course. (A) NL-vifS (black diamonds), NL-4/5S6/7SvifS (white squares), and NL-4/5SG116E6/7SvifS (gray triangles) were inoculated into human CEM-SS cells. Genomic DNA was extracted at the indicated time point post-infection and subjected to real-time PCR assays using U5/gag primers. The number of U5/gag copies per 30 ng of total DNA is indicated. Error bars reflect the SD of triplicate measurements of real-time PCR. Presented data are representative of two independent experiments. (B) VSV-G-pseudotyped GFP-expressing viruses with NL4-3 CA (NL-GFP, black diamonds), 4/5S6/7S CA (NL-4/5S6/7S-GFP, white squares), and 4/5SG116E6/7S CA (NL-4/5SG116E6/7S-GFP, black triangles) were inoculated into human CEM-SS cells. Real-time PCR assays using U5/gag primers were performed as described above. Error bars reflect the SD of triplicate infections. Presented data are representative of three independent experiments.

doi: 10.1371/journal.pone.0072531.g004

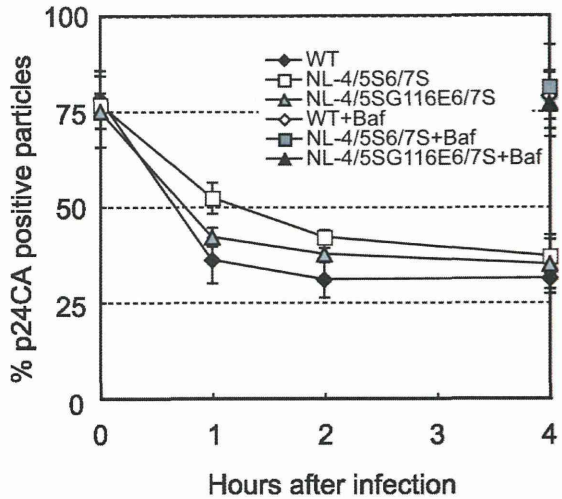

Figure 5. *In situ* uncoating assay. HeLa cells were spinoculated with VSV-G-pseudotyped, S15-dTomato, GFP-Vpr -labeled NL-Nh (WT; black diamonds), NL-Nh with 4/5S6/7S CA (NL-4/5S6/7S, white squares), or NL-Nh with 4/5SG116E6/7S CA (NL-4/5G116E6/7S, gray triangles) for 2 hr at 16° C in the presence or absence of bafilomycin A (BafA). Infection was synchronized by washing off inocula and replacing with 37° *C medium*. At the indicated time post-infection, the cells were fixed, immunostained for p24 CA (Cy-5), and imaged. The identity of the samples was blinded before counting. GFP-positive puncta then were quantified and individually examined for the presence of dTomato and Cy-5 (p24 CA) signals. The percentage of the total number of fused (dTomato-) virions that stained for p24 CA over time following fusion is shown. The 0-hr time point and BafA (+) samples represent total number of GFP-positive virions that stained positive for p24 CA. For BafA treatment, only data from the 4-hr time points on 4/5S6/7S CA (NL-4/5S6/7S+Baf, a grey square), or 4/5SG116E6/7S CA (NL-4/5G116E6/7S+Baf, a black triangle) are shown. The results shown are means and SD from three independent experiments. Actual numbers of counted dots are provided in Table S1.

doi: 10.1371/journal.pone.0072531.g005

and the number of complexes that contained CA (coated) was compared to the number of complexes that lost CA staining (uncoated). The data was graphed at each time point as the % of fused CA-positive (coated) cytoplasmic particles (Figure 5). Actual numbers of counted dots are shown in Table S1. At 1 and 2 hr after infection, virus encoding 4/5S6/7S CA had a higher percentage of CA-positive particles than did the virus encoding NL4-3 CA; the difference was significant (p=0.018 and p=0.018 for 1 and 2 hr, respectively) at each time point. In comparison, virus encoding 4/5SG116E6/7S CA had amounts of CA-positive particles that were not significantly different from those seen with the virus encoding NL4-3 CA (p=0.18 and p=0.08 for 1 and 2 hr, respectively). The differences between 4/5S6/7S and 4/5SG116E6/7S viruses at 1 and 2 hr after infection were small but statistically significant (p=0.021 and p=0.037 respectively). These results suggested that the uncoating kinetics of NL-4/5S6/7SvifS was slower than that of NL-vifS, while the uncoating kinetics of NL-4/5SG116E6/7SvifS was similar to that of NL-vifS.

Discussion

We previously constructed a simian-tropic HIV-1 NL-4/5S6/7SvifS that can replicate well in CM cells [21,22].

However, the replicative capability of this virus in human cells was severely impaired. NL-4/5S6/7SvifS showed nearly normal levels of Gag processing and human TRIM5α sensitivity similar to that of NL4-3 [22]. In the present study, we showed that the amount of RT products of NL-4/5S6/7SvifS was reduced compared to those of NL-vifS at 12 hr after infection. Surprisingly, however, the amount of the RT products of NL-4/5S6/7SvifS at 4 and 8 hr after infection was elevated compared to that of WT. Analysis of 2-LTR and integrated HIV DNA suggested that NL-4/5S6/7SvifS had a defect in nuclear entry but not in integration. By contrast, NL-4/5SG116E6/7SvifS, which encodes a single G116E substitution in CA, showed partial restoration of replicative capability, even though the amount of the RT products was apparently reduced. These results indicated that the G-to-E substitution at the 116th position of CA impaired RT production but restored the defect of NL-4/5S6/7SvifS in the subsequent step.

Mutations in CA have been reported to affect viral core stability, resulting in deleterious effects on RT [4,10] or nuclear entry [12]. In the work described here, VSV-G-pseudotyped virus with NL-4/5S6/7S CA showed slower uncoating kinetics. Thus, it is possible that the hyper-stable core of NL-4/5S6/7SvifS affects nuclear entry, resulting in lower replicative capability in human cells. It remains unclear why the hyper-stable core would be deleterious for nuclear entry. One possible explanation is that the hyper-stable core masks viral nuclear localization signals of matrix, integrase, or Vpr [30–32], or masks a viral DNA structure, the central DNA flap, which is known to be important for nuclear targeting [33–36]. Another possibility is that host factors that are required for HIV-1 to enter the nucleus, such as importin α/importin β heterodimer [37–39], importin 7 [37,40,41], NUP153 [42], and TNPO3 [20], are unable to access the viral particles at the proper time or place. Although TNPO3 has been shown to bind HIV-1 integrase, Krishnan et al. recently showed that CA is the viral factor that dictates TNPO3 dependency [43]. Thus it is also possible that mutations in CA of NL-4/5S6/7SvifS affected the interaction between CA and TNPO3.

It is possible that the core of each HIV-1 CA mutant has its own optimal uncoating kinetics for RT production. For example, a virus with Q63/67A mutations in CA previously has been shown to uncoat more slowly than WT, but could synthesize cDNA at a level comparable to that of WT during single-round infection [4,11,12,44]. In the case of NL-4/5S6/7SvifS, the slow uncoating may be optimal for its RT, since RT production by this virus was faster than that by WT, even though the slower uncoating might be deleterious for nuclear entry. If so, it is reasonable to assume that the G-to-E substitution at the 116th position of CA that reduced the core stability of NL-4/5S6/7SvifS resulted in impaired RT. Further studies, including evaluation of physical core stability and more precise analysis of RT products, are necessary to substantiate this hypothesis.

It is known that drug-resistant HIV-1 often acquires mutations that have a negative effect on viral replicative capability [45–50]. In addition, some of the resistant viruses acquire secondary mutations that do not compensate directly for the negative effects caused by the primary mutations, but instead improve another step, resulting in better replicative capability [51,52]. Similarly, the G-to-E substitution at the 116th position of CA may impair RT production but compensate for a defect of NL-4/5S6/7SvifS in a subsequent step. In the present study, however, we failed to resolve the step at which the G116E substitution of CA compensates for a defect of NL-4/5S6/7SvifS, since no significant improvement was observed in the levels of 2-LTR circles (nuclear entry) nor HIV-Alu (integration) of NL-4/5SG116E6/7S at 12 hr after infection (Figure 3). The addition of the G116E mutation to NL-4/5S6/7SvifS may change the affinity of viral core for certain host factors and subsequently allow viral cDNA to be integrated at chromosome positions that are preferable for subsequent transcription. Alternatively, we might have failed (in Figure 3) to detect very small recoveries of 2-LTR circles and/or HIV-Alu levels, although these recoveries were sufficient to be detected after amplification by viral transcription (in Figure 2). Further studies would be required to elucidate the precise mechanisms by which the G116E mutation at least partially restored the impaired infectivity of NL-4/5S6/7SvifS.

We note that the uncoating process was completed within 4hr after infection (as shown in Figure 5), while the levels of the late-RT products continued to increase through 8-12 hr (as shown in Figures 3 and 4). Similar delay in accumulation of late-RT product compared with uncoating kinetics was reported previously [44]. Since a fluorescence-labeled antibody was used to detect assembled CAs of the pre-uncoating cores in the uncoating assay, it is likely that some cores undergoing uncoating became undetectable in this assay but still continued RT production. At present, the precise role of CA in nuclear entry and integration of HIV-1 remains to be elucidated. Further studies would be needed to determine the number of CA molecules required for efficient nuclear entry and integration of HIV-1 pre-integration complex.

It should be noted here that the amounts of p24 from culture supernatants of 293T cells transfected with NL-4/5S6/7SvifS and NL-4/5SG116E6/7SvifS plasmid constructs were approximately 75% of those of NL-vifS (data not shown). These results suggested that the viral assembly step also is impaired in NL-4/5S6/7SvifS, and that the G-to-E substitution in NL-4/5SG116E6/7SvifS fails to compensate for the mild defect in assembly of NL-4/5S6/7SvifS. Therefore, defects in both early and late viral replication steps may contribute to the impaired replicative capabilities of NL-4/5S6/7SvifS and NL-4/5SG116E6/7SvifS in human cells. It is also possible that NL-4/5S6/7SvifS has defects in steps other than those assessed in the present study.

In the study presented here, we showed that a simian-tropic HIV-1, NL-4/5S6/7SvifS, exhibited both slower uncoating and a defect in nuclear entry. On the other hand, the adapted virus NL-4/5SG116E6/7SvifS showed recovered uncoating kinetics. In addition to the Q63/67A mutant, 4/5S6/7S is the second example showing the association of slower uncoating with a disadvantage in nuclear entry. However, it is too early to generalize from this conclusion, and further studies on various other CA mutants would be required to elucidate the precise role of uncoating kinetics in HIV-1 replication.

Conclusions

Our results suggest that the lower replicative capability of NL-4/5S6/7SvifS in human cells is due to the slower uncoating of this virus.

Supporting Information

Table S1. Actual numbers of dots in uncoating assay.
(DOCX)

Acknowledgements

We are grateful to Cindy Danielson, Doug Dylla, and Z Kelley for their support with the *in situ* uncoating assay. We thank Tadashi Miyamoto for helping with experiments, and Setsuko Bandou and Noriko Teramoto for their assistance. pNL4-3-Luc-R-E- plasmid and AG3.0 antibody to p24CA were obtained through the AIDS Research and Reference Reagent Program, Division of AIDS, NIAID, NIH. NL-Nh and MSMnG plasmid were kind gifts from Dr. Jun-ichi Sakuragi.

Author Contributions

Conceived and designed the experiments: KK EEN TS. Performed the experiments: KK ET HT AK EEN. Analyzed the data: KK ET AEH TJH EEN TS. Contributed reagents/materials/analysis tools: AEH TJH. Wrote the manuscript: KK EEN TS.

References

1. Bukrinsky MI, Sharova N, McDonald TL, Pushkarskaya T, Tarpley WG et al. (1993) Association of integrase, matrix, and reverse transcriptase antigens of human immunodeficiency virus type 1 with viral nucleic acids following acute infection. Proc Natl Acad Sci U S A 90: 6125-6129. doi:10.1073/pnas.90.13.6125. PubMed: 7687060.
2. Fassati A, Goff SP (2001) Characterization of intracellular reverse transcription complexes of human immunodeficiency virus type 1. J Virol 75: 3626-3635. doi:10.1128/JVI.75.8.3626-3635.2001. PubMed: 11264352.
3. Miller MD, Farnet CM, Bushman FD (1997) Human immunodeficiency virus type 1 preintegration complexes: studies of organization and composition. J Virol 71: 5382-5390. PubMed: 9188609.
4. Forshey BM, von Schwedler U, Sundquist WI, Aiken C (2002) Formation of a human immunodeficiency virus type 1 core of optimal stability is crucial for viral replication. J Virol 76: 5667-5677. doi: 10.1128/JVI.76.11.5667-5677.2002. PubMed: 11991995.
5. Fitzon T, Leschonsky B, Bieler K, Paulus C, Schröder J et al. (2000) Proline residues in the HIV-1 NH2-terminal capsid domain: structure determinants for proper core assembly and subsequent steps of early replication. Virology 268: 294-307. doi:10.1006/viro.1999.0178. PubMed: 10704338.
6. Leschonsky B, Ludwig C, Bieler K, Wagner R (2007) Capsid stability and replication of human immunodeficiency virus type 1 are influenced critically by charge and size of Gag residue 183. J Gen Virol 88: 207-216. doi:10.1099/vir.0.81894-0. PubMed: 17170453.
7. Scholz I, Arvidson B, Huseby D, Barklis E (2005) Virus particle core defects caused by mutations in the human immunodeficiency virus capsid N-terminal domain. J Virol 79: 1470-1479. doi:10.1128/JVI.79.3.1470-1479.2005. PubMed: 15650173.
8. Tang S, Murakami T, Agresta BE, Campbell S, Freed EO et al. (2001) Human immunodeficiency virus type 1 N-terminal capsid mutants that exhibit aberrant core morphology and are blocked in initiation of reverse transcription in infected cells. J Virol 75: 9357-9366. doi: 10.1128/JVI.75.19.9357-9366.2001. PubMed: 11533199.
9. Tang S, Murakami T, Cheng N, Steven AC, Freed EO et al. (2003) Human immunodeficiency virus type 1 N-terminal capsid mutants containing cores with abnormally high levels of capsid protein and virtually no reverse transcriptase. J Virol 77: 12592-12602. doi:10.1128/JVI.77.23.12592-12602.2003. PubMed: 14610182.
10. Wacharapornin P, Lauhakirti D, Auewarakul P (2007) The effect of capsid mutations on HIV-1 uncoating. Virology 358: 48-54. doi:10.1016/j.virol.2006.08.031. PubMed: 16996553.
11. Yamashita M, Perez O, Hope TJ, Emerman M (2007) Evidence for direct involvement of the capsid protein in HIV infection of nondividing cells. PLOS Pathog 3: 1502-1510. PubMed: 17967060.
12. Dismuke DJ, Aiken C (2006) Evidence for a functional link between uncoating of the human immunodeficiency virus type 1 core and nuclear import of the viral preintegration complex. J Virol 80: 3712-3720. doi:10.1128/JVI.80.8.3712-3720.2006. PubMed: 16571788.
13. Stremlau M, Perron M, Lee M, Li Y, Song B et al. (2006) Specific recognition and accelerated uncoating of retroviral capsids by the TRIM5alpha restriction factor. Proc Natl Acad Sci U S A 103: 5514-5519. doi:10.1073/pnas.0509996103. PubMed: 16540544.
14. Sayah DM, Sokolskaja E, Berthoux L, Luban J (2004) Cyclophilin A retrotransposition into TRIM5 explains owl monkey resistance to HIV-1. Nature 430: 569-573. doi:10.1038/nature02777. PubMed: 15243629.
15. Sebastian S, Luban J (2005) TRIM5alpha selectively binds a restriction-sensitive retroviral capsid. Retrovirology 2: 40. doi: 10.1186/1742-4690-2-40. PubMed: 15967037.
16. Forshey BM, Shi J, Aiken C (2005) Structural requirements for recognition of the human immunodeficiency virus type 1 core during host restriction in owl monkey cells. J Virol 79: 869-875. doi:10.1128/JVI.79.2.869-875.2005. PubMed: 15613315.
17. Shi J, Aiken C (2006) Saturation of TRIM5 alpha-mediated restriction of HIV-1 infection depends on the stability of the incoming viral capsid. Virology 350: 493-500. doi:10.1016/j.virol.2006.03.013. PubMed: 16624363.
18. Yamashita M, Emerman M (2004) Capsid is a dominant determinant of retrovirus infectivity in nondividing cells. J Virol 78: 5670-5678. doi: 10.1128/JVI.78.11.5670-5678.2004. PubMed: 15140964.
19. Brass AL, Dykxhoorn DM, Benita Y, Yan N, Engelman A et al. (2008) Identification of host proteins required for HIV infection through a functional genomic screen. Science 319: 921-926. doi:10.1126/science.1152725. PubMed: 18187620.
20. Christ F, Thys W, De Rijck J, Gijsbers R, Albanese A et al. (2008) Transportin-SR2 imports HIV into the nucleus. Curr Biol 18: 1192-1202. doi:10.1016/j.cub.2008.07.079. PubMed: 18722123.
21. Kuroishi A, Saito A, Shingai Y, Shioda T, Nomaguchi M et al. (2009) Modification of a loop sequence between alpha-helices 6 and 7 of virus capsid (CA) protein in a human immunodeficiency virus type 1 (HIV-1) derivative that has simian immunodeficiency virus (SIVmac239) vif and CA alpha-helices 4 and 5 loop improves replication in cynomolgus monkey cells. Retrovirology 6: 70. doi:10.1186/1742-4690-6-S2-P70. PubMed: 19650891.
22. Kuroishi A, Bozek K, Shioda T, Nakayama EE (2010) A single amino acid substitution of the human immunodeficiency virus type 1 capsid protein affects viral sensitivity to TRIM5 alpha. Retrovirology 7: 58. doi: 10.1186/1742-4690-7-58. PubMed: 20609213.
23. Nomaguchi M, Yokoyama M, Kono K, Nakayama EE, Shioda T et al. (2013) Gag-CA Q110D mutation elicits TRIM5-independent enhancement of HIV-1mt replication in macaque cells. Microbes Infect 15: 56-65. doi:10.1016/j.micinf.2012.10.013. PubMed: 23123544.
24. Kamada K, Igarashi T, Martin MA, Khamsri B, Hatcho K et al. (2006) Generation of HIV-1 derivatives that productively infect macaque monkey lymphoid cells. Proc Natl Acad Sci U S A 103: 16959-16964. doi:10.1073/pnas.0608289103. PubMed: 17065315.
25. Ohishi M, Shioda T, Sakuragi J (2007) Retro-transduction by virus pseudotyped with glycoprotein of vesicular stomatitis virus. Virology 362: 131-138. doi:10.1016/j.virol.2006.12.030. PubMed: 17258261.
26. Julias JG, Ferris AL, Boyer PL, Hughes SH (2001) Replication of phenotypically mixed human immunodeficiency virus type 1 virions containing catalytically active and catalytically inactive reverse transcriptase. J Virol 75: 6537-6546. doi:10.1128/JVI.75.14.6537-6546.2001. PubMed: 11413321.
27. Vanmaele C, Van Malderen L, Spileers W (2003) The use of a pinhole aperture during the recording of pattern reversal visual evoked potentials. Bull Soc Belge Ophtalmol: 21-27. PubMed: 14750227.

28. Campbell EM, Perez O, Melar M, Hope TJ (2007) Labeling HIV-1 virions with two fluorescent proteins allows identification of virions that have productively entered the target cell. Virology 360: 286-293. doi: 10.1016/j.virol.2006.10.025. PubMed: 17123568.
29. Song H, Nakayama EE, Yokoyama M, Sato H, Levy JA et al. (2007) A single amino acid of the human immunodeficiency virus type 2 capsid affects its replication in the presence of cynomolgus monkey and human TRIM5alphas. J Virol 81: 7280-7285. doi:10.1128/JVI.00406-07. PubMed: 17475650.
30. Bouyac-Bertoia M, Dvorin JD, Fouchier RA, Jenkins Y, Meyer BE et al. (2001) HIV-1 infection requires a functional integrase NLS. Mol Cell 7: 1025-1035. doi:10.1016/S1097-2765(01)00240-4. PubMed: 11389849.
31. Bukrinsky MI, Haggerty S, Dempsey MP, Sharova N, Adzhubel A et al. (1993) A nuclear localization signal within HIV-1 matrix protein that governs infection of non-dividing cells. Nature 365: 666-669. doi: 10.1038/365666a0. PubMed: 8105392.
32. Popov S, Rexach M, Zybarth G, Reiling N, Lee MA et al. (1998) Viral protein R regulates nuclear import of the HIV-1 pre-integration complex. EMBO J 17: 909-917. doi:10.1093/emboj/17.4.909. PubMed: 9463369.
33. Ao Z, Yao X, Cohen EA (2004) Assessment of the role of the central DNA flap in human immunodeficiency virus type 1 replication by using a single-cycle replication system. J Virol 78: 3170-3177. doi:10.1128/JVI.78.6.3170-3177.2004. PubMed: 14990738.
34. Dvorin JD, Bell P, Maul GG, Yamashita M, Emerman M et al. (2002) Reassessment of the roles of integrase and the central DNA flap in human immunodeficiency virus type 1 nuclear import. J Virol 76: 12087-12096. doi:10.1128/JVI.76.23.12087-12096.2002. PubMed: 12414950.
35. Limón A, Nakajima N, Lu R, Ghory HZ, Engelman A (2002) Wild-type levels of nuclear localization and human immunodeficiency virus type 1 replication in the absence of the central DNA flap. J Virol 76: 12078-12086. doi:10.1128/JVI.76.23.12078-12086.2002. PubMed: 12414949.
36. Zennou V, Petit C, Guetard D, Nerhbass U, Montagnier L et al. (2000) HIV-1 genome nuclear import is mediated by a central DNA flap. Cell 101: 173-185. doi:10.1016/S0092-8674(00)80828-4. PubMed: 10786833.
37. Fassati A, Görlich D, Harrison I, Zaytseva L, Mingot JM (2003) Nuclear import of HIV-1 intracellular reverse transcription complexes is mediated by importin 7. EMBO J 22: 3675-3685. doi:10.1093/emboj/cdg357. PubMed: 12853482.
38. Gallay P, Hope T, Chin D, Trono D (1997) HIV-1 infection of nondividing cells through the recognition of integrase by the importin/karyopherin pathway. Proc Natl Acad Sci U S A 94: 9825-9830. doi: 10.1073/pnas.94.18.9825. PubMed: 9275210.
39. Hearps AC, Jans DA (2006) HIV-1 integrase is capable of targeting DNA to the nucleus via an importin alpha/beta-dependent mechanism. Biochem J 398: 475-484. doi:10.1042/BJ20060466. PubMed: 16716146.
40. Ao Z, Huang G, Yao H, Xu Z, Labine M et al. (2007) Interaction of human immunodeficiency virus type 1 integrase with cellular nuclear import receptor importin 7 and its impact on viral replication. J Biol Chem 282: 13456-13467. doi:10.1074/jbc.M610546200. PubMed: 17360709.
41. Zaitseva L, Cherepanov P, Leyens L, Wilson SJ, Rasaiyaah J et al. (2009) HIV-1 exploits importin 7 to maximize nuclear import of its DNA genome. Retrovirology 6: 11. doi:10.1186/1742-4690-6-11. PubMed: 19193229.
42. Woodward CL, Prakobwanakit S, Mosessian S, Chow SA (2009) Integrase interacts with nucleoporin NUP153 to mediate the nuclear import of human immunodeficiency virus type 1. J Virol 83: 6522-6533. doi:10.1128/JVI.02061-08. PubMed: 19369352.
43. Krishnan L, Matreyek KA, Oztop I, Lee K, Tipper CH et al. (2010) The requirement for cellular transportin 3 (TNPO3 or TRN-SR2) during infection maps to human immunodeficiency virus type 1 capsid and not integrase. J Virol 84: 397-406. doi:10.1128/JVI.01899-09. PubMed: 19846519.
44. Hulme AE, Perez O, Hope TJ (2011) Complementary assays reveal a relationship between HIV-1 uncoating and reverse transcription. Proc Natl Acad Sci U S A 108: 9975-9980. doi:10.1073/pnas.1014522108. PubMed: 21628558.
45. Condra JH, Schleif WA, Blahy OM, Gabryelski LJ, Graham DJ et al. (1995) In vivo emergence of HIV-1 variants resistant to multiple protease inhibitors. Nature 374: 569-571. doi:10.1038/374569a0. PubMed: 7700387.
46. Condra JH, Holder DJ, Schleif WA, Blahy OM, Danovich RM et al. (1996) Genetic correlates of in vivo viral resistance to indinavir, a human immunodeficiency virus type 1 protease inhibitor. J Virol 70: 8270-8276. PubMed: 8970946.
47. Croteau G, Doyon L, Thibeault D, McKercher G, Pilote L et al. (1997) Impaired fitness of human immunodeficiency virus type 1 variants with high-level resistance to protease inhibitors. J Virol 71: 1089-1096. PubMed: 8995629.
48. Martinez-Picado J, Savara AV, Sutton L, D'Aquila RT (1999) Replicative fitness of protease inhibitor-resistant mutants of human immunodeficiency virus type 1. J Virol 73: 3744-3752. PubMed: 10196268.
49. Molla A, Korneyeva M, Gao Q, Vasavanonda S, Schipper PJ et al. (1996) Ordered accumulation of mutations in HIV protease confers resistance to ritonavir. Nat Med 2: 760-766. doi:10.1038/nm0796-760. PubMed: 8673921.
50. Zennou V, Mammano F, Paulous S, Mathez D, Clavel F (1998) Loss of viral fitness associated with multiple Gag and Gag-Pol processing defects in human immunodeficiency virus type 1 variants selected for resistance to protease inhibitors in vivo. J Virol 72: 3300-3306. PubMed: 9525657.
51. Myint L, Matsuda M, Matsuda Z, Yokomaku Y, Chiba T et al. (2004) Gag non-cleavage site mutations contribute to full recovery of viral fitness in protease inhibitor-resistant human immunodeficiency virus type 1. Antimicrob Agents Chemother 48: 444-452. doi:10.1128/AAC.48.2.444-452.2004. PubMed: 14742193.
52. Nijhuis M, Schuurman R, de Jong D, Erickson J, Gustchina E et al. (1999) Increased fitness of drug resistant HIV-1 protease as a result of acquisition of compensatory mutations during suboptimal therapy. AIDS 13: 2349-2359. doi:10.1097/00002030-199912030-00006. PubMed: 10597776.

Journal of General Virology (2014), **95**, 179–189 DOI 10.1099/vir.0.057364-0

Poly-proline motif in HIV-2 Vpx is critical for its efficient translation

Ariko Miyake,[1]† Mikako Fujita,[2]† Haruna Fujino,[3] Ryoko Koga,[3] Sogo Kawamura,[3] Masami Otsuka,[3] Hirotaka Ode,[4,5] Yasumasa Iwatani,[4] Yosuke Sakai,[1] Naoya Doi,[1,5] Masako Nomaguchi,[1] Akio Adachi[1] and Yasuyuki Miyazaki[1]

Correspondence
Akio Adachi
adachi@basic.med.tokushima-u.ac.jp
Yasuyuki Miyazaki
ymiyazaki@basic.med.tokushima-u.ac.jp

[1]Department of Microbiology, Institute of Health Biosciences, University of Tokushima Graduate School, Tokushima, Tokushima, Japan

[2]Research Institute for Drug Discovery, School of Pharmacy, Kumamoto University, Kumamoto, Kumamoto, Japan

[3]Department of Bioorganic Medicinal Chemistry, Faculty of Life Sciences, Kumamoto University, Kumamoto, Kumamoto, Japan

[4]Clinical Research Center, National Hospital Organization, Nagoya Medical Center, Nagoya, Aichi, Japan

[5]Japanese Foundation for AIDS Prevention, Chiyoda-ku, Tokyo, Japan

Human immunodeficiency virus type 2 (HIV-2) carries an accessory protein Vpx that is important for viral replication in natural target cells. In its C-terminal region, there is a highly conserved poly-proline motif (PPM) consisting of seven consecutive prolines, encoded in a poly-pyrimidine tract. We have previously shown that PPM is critical for Vpx expression and viral infectivity. To elucidate the molecular basis underlying this observation, we analysed the expression of Vpx proteins with various PPM mutations by *in vivo* and *in vitro* systems. We found that the number and position of consecutive prolines in PPM are important for Vpx expression, and demonstrated that PPM is essential for efficient Vpx translation. Furthermore, mutational analysis to synonymously disrupt the poly-pyrimidine tract suggested that the context of PPM amino acid sequences is required for efficient translation of Vpx. We similarly analysed HIV-1 and HIV-2 Vpr proteins structurally related to HIV-2 Vpx. Expression level of the two Vpr proteins lacking PPM was shown to be much lower relative to that of Vpx, and not meaningfully enhanced by introduction of PPM at the C terminus. Finally, we examined the Vpx of simian immunodeficiency virus from rhesus monkeys (SIVmac), which also has seven consecutive prolines, for PPM-dependent expression. A multi-substitution mutation in the PPM markedly reduced the expression level of SIVmac Vpx. Taken together, it can be concluded that the notable PPM sequence enhances the expression of Vpx proteins from viruses of the HIV-2/SIVmac group at the translational level.

Received 16 July 2013
Accepted 9 October 2013

INTRODUCTION

Primate immunodeficiency viruses carry a set of accessory proteins necessary for their optimal growth in host individuals (Blanco-Melo *et al.*, 2012; Harris *et al.*, 2012; Malim & Bieniasz, 2012; Zheng *et al.*, 2012). Extensive virological and molecular biological studies carried out so far have revealed that these auxiliary proteins profit the viruses mostly by antagonizing cellular antiviral restriction factors (Blanco-Melo *et al.*, 2012; Harris *et al.*, 2012; Malim & Bieniasz, 2012; Zheng *et al.*, 2012). One such viral protein, Vpx, is highly conserved among viruses of the human immunodeficiency virus type 2 (HIV-2) group, and plays a critical role in viral replication in different cell types (Fujita *et al.*, 2010). Vpx produced in cells is subsequently incorporated into progeny virions through a specific interaction of the putative third α-helix region (Jin *et al.*, 2001; Park & Sodroski, 1995) with the p6 domain of Gag (Accola *et al.*, 1999; Pancio & Ratner, 1998). The packaged Vpx then confers optimal infectivity on the virions in specific target cells such as macrophages and primary T-cells. Recently, it has been demonstrated that Vpx induces proteasomal degradation of host factors SAMHD1 (Hrecka *et al.*, 2011; Laguette *et al.*, 2011) and APOBEC3A (Berger *et al.*, 2011), relieving the restriction of virus infection.

†These authors contributed equally to this work.

Vpx presumably has three major α-helices and unstructured amino/carboxy termini like its paralogue Vpr (Khamsri *et al.*, 2006; Mahnke *et al.*, 2006), another accessory protein known to be abundantly virion-associated. Despite this similarity, there is a notable poly-proline motif (PPM) near the C terminus of Vpx (seven consecutive prolines in the Vpx proteins of HIV-2; simian immunodeficiency virus from rhesus monkeys, SIVmac; and SIV from sooty mangabey monkeys, SIVsmm), which is not present in Vpr. We have previously generated a series of proviral HIV-2 mutant clones and performed systemic virological studies on Vpx using primary macrophage cultures and a T-lymphocyte cell line as infection targets (Fujita *et al.*, 2008a, b, 2010; Ueno *et al.*, 2003). Although all 19 point mutants, with mutations scattered throughout the *vpx* gene, produced virions containing Vpx at a comparable level to a WT clone upon transfection, many of them were found to be defective for virus growth in macrophages and/or T-cells. The defective replication step of these mutants was shown to be in the early phase (before/during viral DNA synthesis and/or its nuclear import) by extensive virological and molecular analyses (Fujita *et al.*, 2008a, b, 2010; Ueno *et al.*, 2003). In contrast to above, the other two multi-substitution mutants of the proline stretch designated 103/4A and 106/4A (Fig. 1a) failed to express Vpx upon transfection and produced progeny virions without detectable Vpx (Fujita *et al.*, 2008a, b). Consistently, the two mutant viruses were growth-defective both in macrophages and T-cells (Fujita *et al.*, 2008b). In particular, the 106/4A mutant virus behaved exactly like a ΔVpx virus in infection experiments (Table 1). Although severely impeded, the 103/4A mutant virus was still infectious for macrophages and T-cells (Table 1). Because the expression of 103/4A and 106/4A Vpx proteins was below the detection level of the system used (Table 1), the reason for the different growth abilities of the two viruses remained to be determined. Notably, it has been shown that a PPM-deletion mutant, if expressed to some extent, retains Vpx functionality in single-round infection experiments (Goujon *et al.*, 2008; Gramberg *et al.*, 2010).

In this study, we have focused on the role of the PPM in Vpx expression and analysed the underlying molecular basis. Expression plasmids of HIV-2 Vpx with the PPM mutations were constructed for quantitative comparison and utilized for protein expression analysis using various cellular and *in vitro* cell-free translation systems. Our results demonstrated that the PPM in HIV-2 Vpx is critical for its efficient expression in the eukaryotic as well as prokaryotic translation machineries. In addition, we found that this effect is determined by the context of PPM amino acid sequences, but not the nucleotide sequences. These data support the notion that the PPM plays an important role in enhancing the translational level of HIV-2 Vpx in infected cells, thereby conferring optimal replication ability on the virus in target cells.

RESULTS

PPM in Vpx is critical for its efficient expression in cells

We have previously shown that the expression of Vpx in PPM mutants carrying P103/4A or P106/4A is at an undetectable level both in cells and in progeny virions produced from transiently transfected cells (Table 1). However, while the 106/4A mutant virus exhibited a ΔVpx growth-like phenotype in lymphocytic HSC-F cells and no viral growth in macrophages, the 103/4A mutant virus grew better in both cell types than the ΔVpx virus (Table 1). These results led us to assume that the expression plasmid, pME18Neo-Fvpx, used in the study (Fujita *et al.*, 2008b) was unable to efficiently express the protein. Therefore, we have constructed a new expression plasmid based on pEF1/*myc*-HisA (pEF-Fvpx in Fig. 1b), and compared its ability with the old version (pME18Neo-Fvpx in Fig. 1b). As clearly observed in Fig. 1(b), pEF-Fvpx was much more efficient at producing Vpx than pME18Neo-Fvpx upon transfection.

A series of mutants based on pEF-Fvpx were then constructed (Fig. 1a, c, e) and examined for their expression. First, we monitored the expression level of the 103/4A and 106/4A mutants to see if there is a significant difference that can account for the distinct growth phenotype of viruses carrying these mutations (Table 1). As shown in Fig. 1(c), only a faint amount of Vpx was detected for the 106/4A mutant and a deletion mutant lacking the entire PPM-coding region (d7P). Although considerably reduced relative to the WT clone, the 103/4A mutant clearly generated more Vpx than the 106/4A mutant. This result correlated well with the growth potentials of the WT, 103/4A, and 106/4A viruses (Table 1). Next, we determined the effect of the number and position of the alanine substitutions in PPM on Vpx expression (Fig. 1d). A single substitution of proline with alanine did not cause major reductions except for P106A (approximately 50 % of the WT level). Double and triple alanine substitutions gave distinct results. While the P104/2A, P103/3A and P105/3A mutations did not have a significant effect, the expression level of P107/3A relative to that of WT markedly decreased (similar to the P103/4A level). The P106/2A and P108/2A mutants expressed Vpx at a slightly reduced level as observed for P106A. The results in Fig. 1(c, d) showed that the number and position of consecutive prolines in PPM are important for Vpx expression. In addition to the PPM mutations, we analysed the mutational effect of the glycine-rich domain (GRD), which is a presumably flexible region just upstream of PPM (Fig. 1a). In general, poly-proline sequences form a rigid structure whereas glycine repeats provide flexibility. Therefore, we speculated that the GRD may affect the ability of PPM to enhance Vpx expression. However, the introduction of alanine substitutions into the GRD showed no appreciable effects (Fig. 1e).

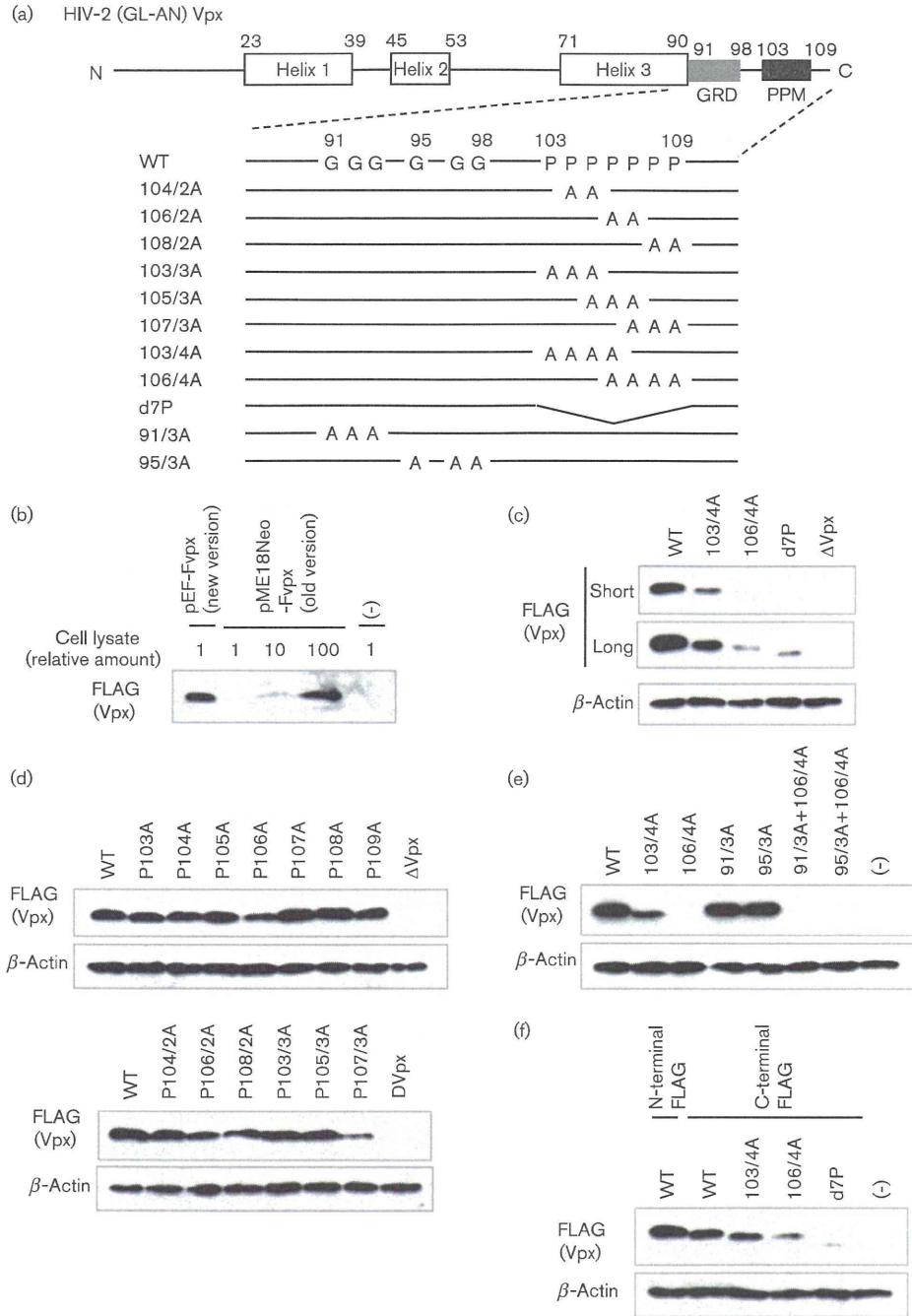

Fig. 1. Expression profiles of various Vpx–PPM mutants in transfected 293T cells. (a) A scheme of the domain structure and sequences of HIV-2 GL-AN Vpx (112 amino acids) and its mutants. Expression plasmids with N-terminal (pEF-Fvpx series)/C-terminal (pEF-vpxF series) FLAG were constructed in this study. Numbers indicate the positions of amino acid residues in the HIV-2 Vpx. GRD, glycine-rich domain; PPM, poly-proline motif. (b) Expression of Vpx from two expression plasmids designated pEF-Fvpx (this study) and pME18Neo-Fvpx (Fujita *et al.*, 2008a, b; Khamsri *et al.*, 2006). Relative amount of cell lysates used for Western blotting is indicated. (c) Expression of Vpx–PPM mutants carrying four successive alanine substitutions or a deletion. Short, short exposure; long, long exposure. (d) Expression of Vpx–PPM mutants carrying a single alanine substitution (upper) or two/three alanine substitutions (lower). (e) Expression of Vpx–GRD mutants with or without the 106/4A mutation. (f) Expression of Vpx–PPM mutants with a C-terminal FLAG tag. (-), pEF1/*myc*-HisA; WT, pEF-Fvpx or pEF-vpxF; ΔVpx, pEF-FxSt.

Table 1. Effect of mutations in HIV-2 GL-AN Vpx on its expression level and viral replication ability

Results obtained in 293T cells, lymphocytic HSC-F cells, and monocyte-derived macrophage (MDM) cultures (Fujita *et al.*, 2008a, b) are summarized.

Clone	Mutation*	Vpx expression†		Viral replication‡	
		Cells	Virions	HSC-F	MDM
GL-AN	None (WT)	WT	WT	WT	WT
GL-St	ΔVpx	UD	UD	ΔVpx	UD
GL-xP103A	P103A	WT	ND	WT	WT
GL-x103/4A	P103/4A	UD	UD	M	M
GL-x106/4A	P106/4A	UD	UD	ΔVpx	UD
GL-xP109A	P109A	WT	ND	WT	M

*ΔVpx, a frame-shift mutation in the *vpx* gene (Kawamura *et al.*, 1994); see Fig. 1 for P103A, P103/4A, P106/4A and P109A mutations.
†WT, wt level expression; UD, undetectable; ND, not done. Vpx proteins in transfected 293T cells (cells) and in virions prepared from transfected 293T cells (virions) were monitored. Vpx in cells was examined by using proviral clones and/or FLAG-tagged Vpx-expression vectors.
‡WT, similar replication to wt virus; ΔVpx, similar replication to GL-St virus; UD, undetectable; M, medium replication phenotype between WT and GL-St viruses.

Although our data here on the 103/4A and 106/4A mutants were consistent with the viral growth properties (Table 1), we asked whether there is a positional effect of the FLAG tag on the Vpx expression. Expression plasmids with a C-terminal FLAG tag based on pEF1/*myc*-HisA (pEF-vpxF constructs: WT, 103/4A, 106/4A and d7P) were constructed, and their ability to express Vpx upon transfection was analysed. As shown in Fig. 1(f), the data obtained were quite similar to those in N-terminal FLAG-tagged vectors. However, the difference in the expression level between clones appeared to be smaller (Fig. 1c, f). This might result from the adjacent effect of the C-terminal FLAG tag on PPM. We used N-terminal tagged versions (pEF-Fvpx clones) thereafter.

PPM facilitates translation of Vpx in a nucleotide sequence-independent manner

The results presented so far indicated that PPM is important for Vpx expression in cells. To further understand the mechanism underlying this observation, we compared the transcription and translation efficiencies of WT and PPM mutants (Fig. 2). We firstly measured mRNA levels in cells transfected with WT or three PPM mutants (103/4A, 106/4A and d7P). Total RNA was extracted from cells and relative *vpx* mRNA level was quantified by the real-time reverse-transcription-PCR (RT-PCR) method. As shown in Fig. 2(a), mutations in PPM did not significantly change the steady-state level of each mRNA in transfected cells. In agreement with this observation, the *in vitro* transcription assay gave similar results (Fig. 2a). However, when the Vpx proteins were synthesized by an *in vitro* transcription/translation system using rabbit reticulocyte lysates, the three PPM mutants were scarcely produced (Fig. 2b). In parallel with the data obtained in transfected cells, the amount of synthesized 103/4A was confirmed to be higher than that of 106/4A in independently repeated experiments (data not shown). Furthermore, we compared the translation efficiency of WT and 106/4A clones by an *in vitro* transcription/translation system using *Escherichia coli* S30 lysates. As seen in Fig. 2(b), the PPM mutation almost abrogated the translation of Vpx even in the bacterial system.

Then, we asked whether the effect of PPM on Vpx translation is linked to the unique secondary structure and/or poly-pyrimidine tract of mRNA around the PPM-coding region (Fig. 3a). At first, mutant plasmids carrying a stop codon just upstream of PPM (G102St and +103St) were constructed (Fig. 3a), and the expression of these mutant proteins was examined in transfected cells as well as in the cell-free system using rabbit reticulocyte lysates. The truncated mutants, G102St and +103St, migrated faster than WT Vpx and were expressed at a much lower level (Fig. 3b). This was also observed in the cell-free system (Fig. 3b). These results suggested that the amino acid sequences of PPM, but not the context of the RNA sequence, are essential for efficient translation of Vpx. Moreover, we constructed various clones with synonymous mutations (106/3ccg, 106/3cca, 105ccg, 106ccg, 107ccg and 104,106ccg) that potentially disrupt the poly-pyrimidine tract (Fig. 3a), and examined their expression levels in transfected cells and in the cell-free system. As shown in Fig. 3(c), the synonymous mutants were expressed as efficiently as WT Vpx. These data also indicated that the role of Vpx PPM is primarily determined by the context of the amino acid sequences, but not by that of nucleotide sequences. Taken together (Figs 2 and 3), our findings showed that the consecutive proline residues of PPM play an essential role in efficient translation of HIV-2 Vpx both in the eukaryotic and prokaryotic systems.

PPM of HIV-2 Vpx does not have a major effect on the expression level of HIV Vpr proteins

Vpx shares many properties with Vpr including virion-association, putative three-dimensional structure, and biological activities (Fujita *et al.*, 2010). However, no PPM is present in HIV-1 and HIV-2 Vpr proteins (Khamsri *et al.*, 2006). In addition, the stoichiometry of Vpx in the virion is much higher than that of Vpr (Singh *et al.*, 2000). Approximately 4000 Vpx are estimated to be packaged in one virion, while only 14–18 HIV-1 Vpr are encapsidated. In accordance with this observation, it has been previously reported that the expression level of HIV Vpr proteins in cells is low relative to that of HIV-2 Vpx as monitored by tagged

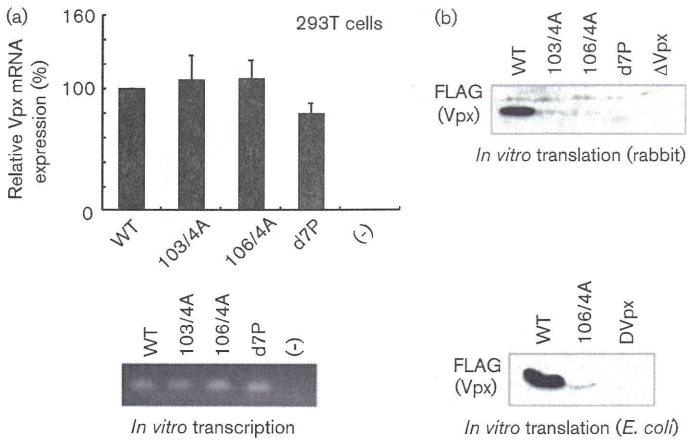

Fig. 2. Effect of PPM mutations on the expression of Vpx mRNA and protein. (a) Upper: relative amounts of Vpx mRNAs in transfected 293T cells. Total RNA was extracted from cells transfected with the expression plasmids indicated at 24 h post-transfection, and subjected to quantitative real-time RT-PCR analysis. Relative copy numbers are shown. (-), pEF1/*myc*-HisA. Lower: amounts of *in vitro* transcribed mRNAs for Vpx. (-), pEF1/*myc*-HisA. (b) Expression of Vpx–PPM mutants by an *in vitro* transcription/translation system using rabbit reticulocyte lysates (upper) or *E. coli* S30 lysates (lower). *, Non-specific bands; WT, pEF-Fvpx or pET-Fvpx; ΔVpx, pEF-FxSt or pET-FxSt.

expression plasmids/tagged proviral clones (Goujon *et al.*, 2008; Gramberg *et al.*, 2010; Khamsri *et al.*, 2006). Based on these results, we speculated that the addition of the HIV-2 Vpx PPM onto HIV-1/HIV-2 Vpr might enhance their expression.

We firstly compared expression levels of mRNA and protein for Vpx and Vpr. The mRNA levels for HIV-1 and HIV-2 Vpr proteins relative to that for HIV-2 Vpx in transiently transfected cells were measured by quantitative RT-PCR. As shown in Fig. 4(a), both Vpr mRNAs, HIV-1 Vpr in particular, were expressed to a lesser extent relative to Vpx mRNA. However, no major difference was noticed for Vpx and Vpr RNAs synthesized *in vitro* (Fig. 4a), probably due to T7 RNA polymerase in the reaction. When the protein expression levels were compared, more drastic results were obtained. HIV-1 and HIV-2 Vpr proteins were scarcely detectable in transfected cells and in the cell-free system (Fig. 4b), in contrast to Vpx. These results suggested that both transcription and translation processes are inefficient for Vpr expression. We then tested whether the PPM augments expression levels of HIV-1 and HIV-2 Vpr proteins by addition of the C-terminal flexible region of HIV-2 Vpx containing the PPM (Vpr1/Vpx and Vpr2/Vpx in Fig. 4c). In transfected cells, both Vpr1/Vpx and Vpr2/Vpx exhibited slightly higher expression relative to parental Vpr1 and Vpr2 clones, respectively (Fig. 4c). However, their expression levels obtained by adding the PPM were still much lower than that of Vpx. In addition, the *in vitro* transcription/translation analysis by rabbit reticulocyte lysates also gave little effect of the substitution with C-terminal flexible region on the translation efficiency (data not shown). These results showed that the addition of the Vpx PPM does not cause a major effect on the expression level of HIV Vpr proteins *in vivo* and *in vitro*.

SIVmac Vpx has PPM consisting of a hepta-proline stretch and its expression is PPM-dependent

For detailed analysis of Vpx and PPM-containing Vpr proteins, we generated a phylogenetic tree of various Vpx/Vpr proteins using SIVsyk (SIV from Sykes' monkeys) Vpr (without PPM) as a reference (Fig. 5). The Vpr of SIV from African green monkeys (SIVagm) has been suggested as an origin of Vpx (Sharp *et al.*, 1996). Notably, the Vpr of SIVagm clone GRI1677 has a PPM composed of five consecutive prolines, and its expression level is markedly reduced as a result of PPM-deletion (data not shown). The PPM (four consecutive prolines) of SIVmnd2 Vpx is located at a relatively similar position (106th to 109th proline) to our Vpx clone (HIV2 GL-AN in Fig. 5). Substitution mutations in this region (P106/4A) almost abolished Vpx expression (Fig. 1). Among various Vpr/Vpx proteins in Fig. 5, other than HIV-2 Vpx, Vpx proteins of SIV from drills (SIVdrl), SIVsmm and SIVmac have seven consecutive prolines.

Based on the results summarized above, we asked whether the P106/4A mutation in the Vpx–PPM of SIVmac gives an effect similar to that observed for HIV-2 Vpx (Fig. 1). As shown in Fig. 6(a), the sequence homology between the two proteins is quite high, the N-terminal half in particular, and the PPM is conserved as described above. Unexpectedly, the amount of SIVmac Vpx produced upon transfection was found to be significantly lower relative to that of HIV-2 Vpx (Fig. 6b). However, as clearly observed, the PPM mutant protein of SIVmac Vpx (106/4A) was expressed at a very reduced level relative to WT Vpx (Fig. 6b), indicating the presence of PPM-dependent regulation. We were interested in mapping the determinant(s) responsible for the different expression levels seen for HIV-2 and SIVmac Vpx proteins. Three chimeric expression plasmids were constructed, and monitored for their expression upon transfection (Fig. 6c). Since the three chimeric constructs expressed Vpx at a similarly low level to the WT SIVmac clone, the putative helix 1 in Vpx was considered to be the determinant. We substituted four amino acids in HIV-2 Vpx helix 1 with corresponding residues in the helix 1 of SIVmac Vpx (Fig. 6a, c). Expectedly, as is clear in Fig. 6(c), the mutant with the four substitutions (GL-D26N/I29V/A31E/L32I) and the WT SIVmac clone produced Vpx at a similarly low level upon

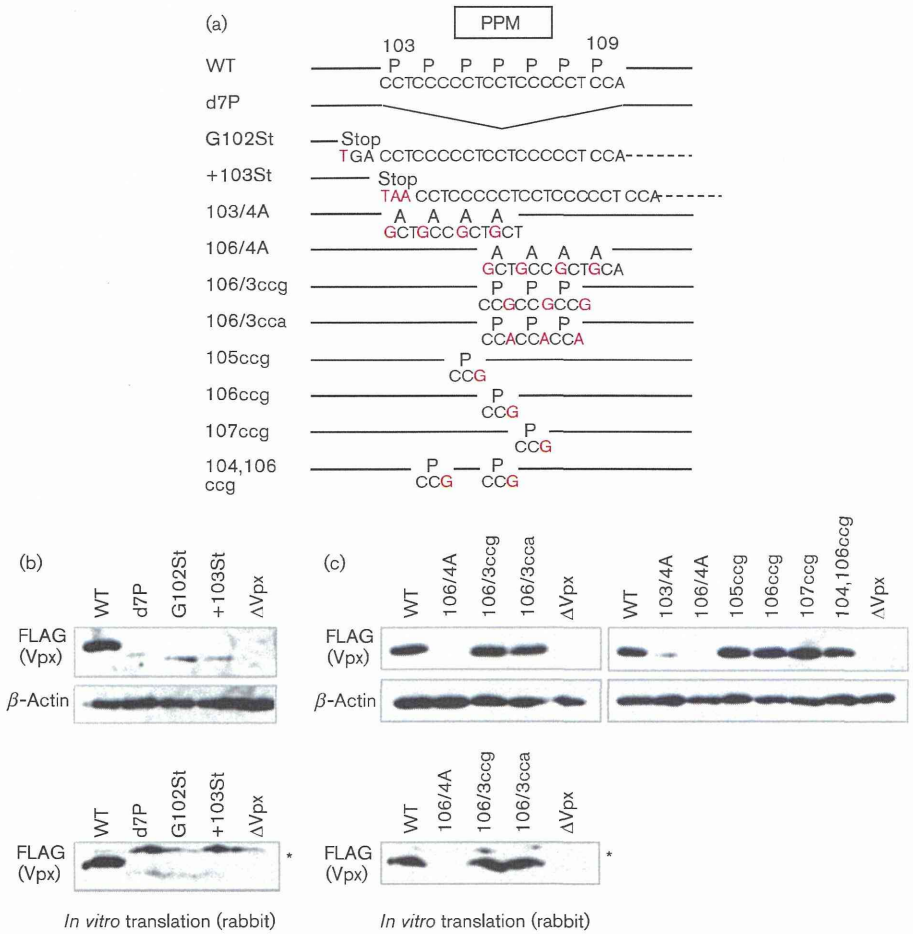

Fig. 3. Effect of poly-pyrimidine tract mutations on Vpx expression. (a) Sequences of the PPM region of WT and mutant clones. Red letters indicate nucleotides changed by mutagenesis. (b, c) Expression profiles of various Vpx–PPM mutants. Samples were prepared from transfected 293T cells (upper) or by an *in vitro* transcription/translation system using rabbit reticulocyte lysates (lower). *, Non-specific bands; WT, pEF-Fvpx; ΔVpx, pEF-FxSt.

transfection. Our results described above showed that the PPM-function itself, i.e., enhancing the Vpx expression level, is maintained in the HIV-2/SIVmac group.

DISCUSSION

One of the most prominent features for Vpx proteins of the HIV-2/SIVsmm/SIVmac group is a highly conserved PPM consisting of a hepta-proline stretch in the C-terminal region (Fig. 5). Our previous studies showed that the PPM in HIV-2 Vpx is required for Vpx expression in cells and virions (Fujita *et al.*, 2008a, b). To gain mechanistic insights into the PPM-dependent Vpx expression, we performed a systemic mutational analysis. We found that each proline residue in PPM is not equally important for Vpx expression, but that the number and position of consecutive proline residues are critical (Fig. 1). Our data showed that at least four consecutive prolines are needed to impose a clear PPM-dependency on Vpx expression. Three (or perhaps two) consecutive prolines were effective if located at the C-terminal half of PPM. Quantitative real-time RT-PCR and *in vitro* transcription/translation assays revealed that the PPM is essential for efficient translation of Vpx in both the eukaryotic and prokaryotic systems (Fig. 2). Moreover, we showed that the stretch of PPM amino acid sequence, but not the nucleotide context, is required for enhancing translation (Fig. 3).

Our data on the expression level of Vpx–PPM mutants in cells (Fig. 1) were well correlated with the ability of mutant viruses to grow in primary macrophages and lymphocytic HSC-F cells (Table 1). While mutant viruses with ability to produce Vpx at a normal level (P103A and P109A) grew comparably

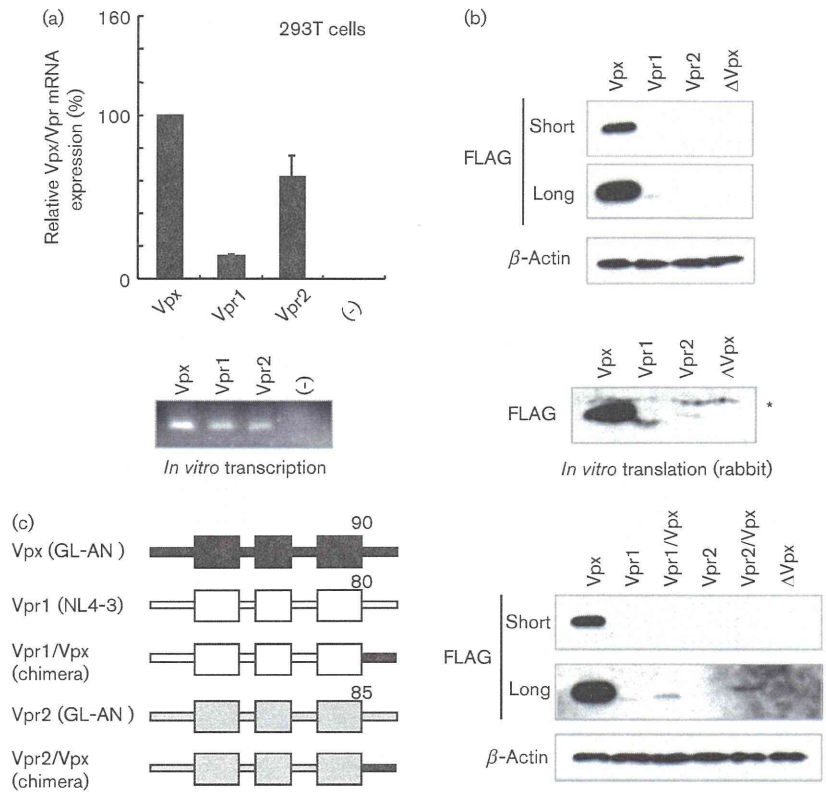

Fig. 4. Expression profiles of HIV Vpx/Vpr mRNAs and proteins. (a) Upper: expression level of Vpx/Vpr mRNAs in transfected 293T cells. Cells were transfected with the expression plasmids for HIV-2 Vpx (Vpx), HIV-1 Vpr (Vpr1) or HIV-2 Vpr (Vpr2). Total RNA was extracted at 24 h post-transfection, and subjected to quantitative real-time RT-PCR analysis with a primer set for the 3′ untranslated region of pEF1/*myc*-HisA-based vectors. Relative copy numbers are shown. (-), pEF1/*myc*-HisA. Lower: *in vitro* transcription by T7 RNA polymerase. Linearized plasmids were used as DNA templates for this assay. (-), pEF1/*myc*-HisA. (b) Upper: expression of Vpx and HIV-1/HIV-2 Vpr proteins in transfected 293T cells. Lower: expression of Vpx and HIV-1/HIV-2 Vpr proteins by an *in vitro* transcription/translation system using rabbit reticulocyte lysates. *, Non-specific bands. (c) Left: schematic structure of chimeric proteins between HIV-2 Vpx (black), HIV-1 Vpr (white), and HIV-2 Vpr (grey) proteins. Numbers indicate amino acid positions at the end of the putative third α-helix. Right: expression of Vpx/Vpr chimeric proteins in transfected 293T cells. Short, Short exposure; long, long exposure; ΔVpx, pEF-FxSt.

with parental WT virus in both cell types, a mutant (103/4A), which expresses a small amount of Vpx, grew very poorly in those cells (Fig. 1, Table 1). A mutant (106/4A), which expresses a negligible amount of Vpx, was unable to grow in macrophages and grew similarly poorly to the ΔVpx mutant virus in HSC-F cells (Fig. 1, Table 1). These results suggested that the PPM is critical for Vpx expression but not for its activity. Functionality, i.e. the potential to confer infectivity on virions, of a PPM-deletion mutant and of a Vpx/Vpr chimeric clone lacking the PPM support this conclusion (Goujon *et al.*, 2008; Gramberg *et al.*, 2010).

Very recently, it has been reported that translation elongation factor P (EF-P) is linked to the adjustment of translational efficiency for poly-proline-containing proteins in the bacterial system (Doerfel *et al.*, 2013; Ude *et al.*, 2013). During the translation, poly-proline stretch sequences tend to induce ribosome stalling, which is likely to be rescued by the EF-P (Doerfel *et al.*, 2013; Ude *et al.*, 2013). It has been reported that eIF5A, like its orthologue EF-P in the bacterial system, promotes translation of PPM-containing proteins in the yeast system (Gutierrez *et al.*, 2013). These results demonstrate the suppressive effect of poly-proline sequences on translation in cells. In contrast, our present study showed that the PPM of HIV-2 Vpx contributes to the enhancement of Vpx translation (Figs 2 and 3) and that the translational enhancement of Vpx occurs in both prokaryotic and eukaryotic machineries. How can we rationalize such opposite effects of poly-proline sequences on translation? At this moment, we do not have the answer but might assume that the HIV-2 PPM could hijack the functions of EF-P and/or eIF5A, which are the factors that stimulate the peptidyltransferase activity of the ribosome. Otherwise,

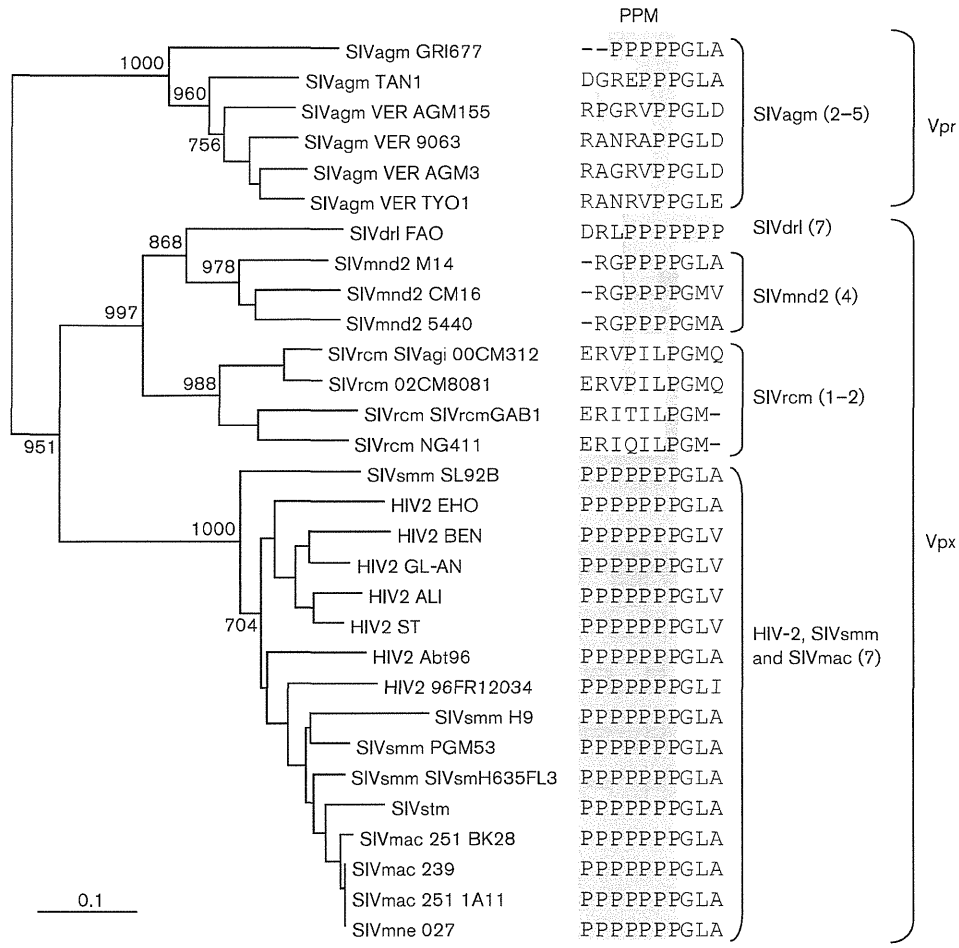

Fig. 5. Phylogenetic analysis of various Vpx and Vpr proteins. Phylogenetic tree was generated by the neighbour-joining method. The genetic distance corresponding to the lengths of branches is shown by the scale bar. Branches were calculated from 1000 bootstrap replicates, and the bootstrap values are labelled on the major branches. Amino acid sequences of the PPM region and numbers of proline residues in parentheses are shown on the right.

an additional unidentified factor(s) important for PPM-mediated protein expression may exist in cells. Moreover, of note, PPM alone did not enhance the synthesis of Vpr proteins in our present study (Fig. 4). Consistently, Vpr engineered to have the C-terminal flexible region of Vpx exhibited inefficient expression in cells, indicating that the PPM alone is insufficient for promoting protein translation (Gramberg *et al.*, 2010). There may be a region(s) and/or amino acids in Vpx other than the PPM sequence important for PPM-dependent efficient translation of Vpx. The putative helix 1 in Vpx was shown to be important for fixing its expression level in cells, but the effect of helix 1 appeared to be independent of the PPM-regulation (Fig. 6). Further study is required to elucidate the molecular mechanism for the PPM-dependent translation enhancement of Vpx.

The PPM sequence is found in a large number of prokaryotic and eukaryotic proteins (UniProt Knowledgebase, http://www.uniprot.org). As expected, a wide range of human DNA and RNA viruses encode PPM (seven or more consecutive prolines)-containing proteins. Examples include adenoviruses, herpesviruses and hepatitis viruses. However, whether these PPMs are responsible for efficient expression of the PPM-containing proteins is as yet undetermined. Extensive studies on these proteins remain to be performed to have a general picture of PPM-mediated protein expression. This paper is the first report, to the best of our knowledge, that describes and demonstrates the PPM-dependent efficient translation of animal virus proteins. Furthermore, we have shown the minimal requirements constituting a 'functional PPM' as described above (Figs 1 and 4). In HIV/SIVs, PPM sequence is also intriguing from an evolutional point of view

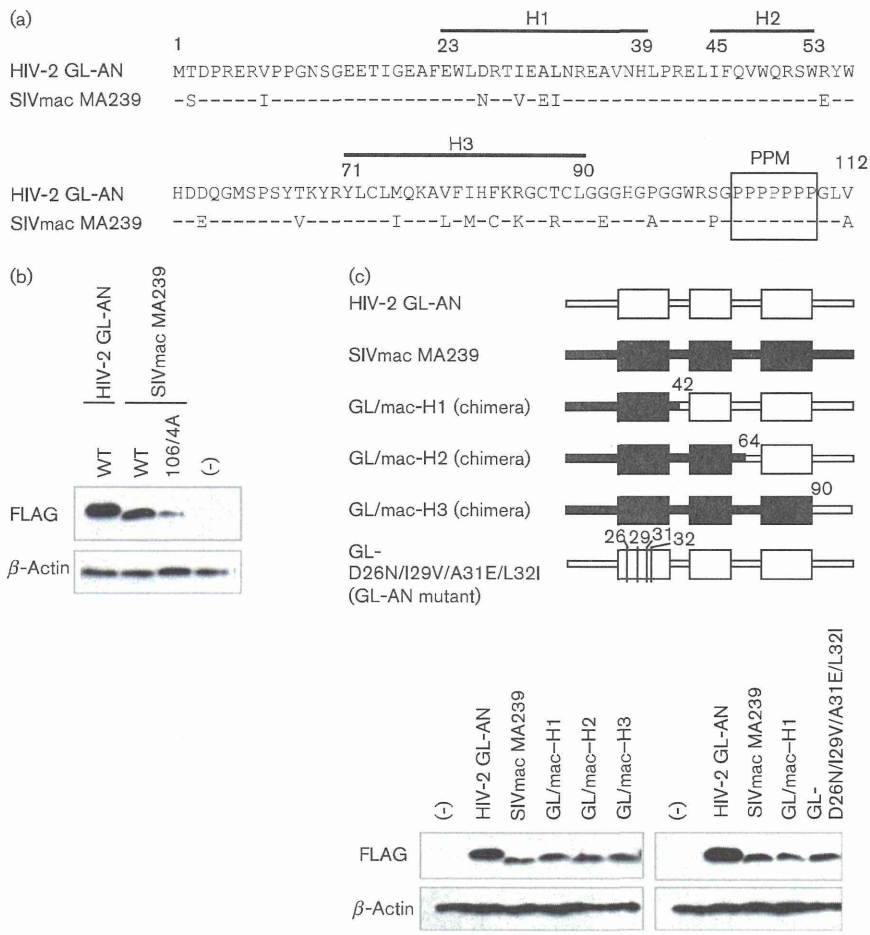

Fig. 6. Expression profiles of various SIVmac and HIV-2 Vpx proteins. (a) Sequence alignment of HIV-2 GL-AN (Kawamura *et al.*, 1994) and SIVmac MA239 (Shibata *et al.*, 1991) Vpx proteins. Numbers indicate the positions of amino acid residues in Vpx. Different amino acids in the putative first α-helix (H1) of HIV-2 GL-AN and SIVmac MA239 Vpx proteins are shaded. (b) Expression of an SIVmac Vpx–PPM mutant carrying four successive alanine substitutions at amino acids 106–109 (P106/4A) in transfected 293T cells. (c) Upper: schematic structure of chimeric proteins between HIV-2 Vpx (white) and SIVmac Vpx (black) proteins. A clone with four mutations relative to HIV-2 GL-AN Vpx is also shown. Numbers indicate the positions of amino acid residues. Lower: expression of HIV-2/SIVmac chimeric Vpx proteins and an HIV-2 mutant Vpx protein in transfected 293T cells. (-), pEF1/*myc*-HisA.

(Fig. 5). HIV-1/HIV-2 Vpr proteins without a PPM were found to be expressed at an extremely low level relative to HIV-2 Vpx (Fig. 4). While the PPM-dependent enhancement was also true for the expression of SIVmac Vpx (Fig. 6) and SIVagm Vpr (our unpublished data), some SIV Vpx/Vpr proteins lack a typical PPM sequence (three, four or more consecutive prolines) (Fig. 5). Although many of the Vpx/Vpr proteins in Fig. 5 are unanalysed to date for the function and expression, it is not unreasonable to assume that each virus in Fig. 5, during its persistent infection in its natural host, has acquired appropriate Vpx and/or Vpr for optimal viral replication and maybe for viral persistence/spread. It would be, therefore, of interest to perform functional and virological studies on the Vpx/Vpr proteins with/without PPM derived from a variety of HIV/SIVs. Studies in this direction are in progress in our laboratory.

METHODS

Plasmids. Expression plasmids for HIV-2 Vpx (GL-AN clone) (Kawamura *et al.*, 1994) with an N-terminal FLAG tag designated pME18Neo-Fvpx and its mutant derivatives have been previously described (Fujita *et al.*, 2008a, b; Khamsri *et al.*, 2006). New plasmids for various Vpx proteins with an N-terminal FLAG, pEF-F series, were constructed by introduction of an appropriate *vpx* gene fragment into pEF1/*myc*-HisA (Life Technologies). The resultant plasmids for WT and its frame-shift mutant (ΔVpx) were designated pEF-Fvpx and pEF-FxSt, respectively. Expression plasmids for HIV-1 Vpr (NL4-3 clone) (Adachi *et al.*, 1986) and HIV-2 Vpr (GL-AN),

designated pEF-Fvpr1 and pEF-Fvpr2, respectively, were constructed by replacement of the *vpx* gene in pEF-Fvpx with each *vpr* gene. Expression plasmids for Vpx/Vpr chimeras were generated by PCR-based mutagenesis using pEF-Fvpx, pEF-Fvpr1 and pEF-Fvpr2. To construct an expression plasmid for HIV-2 Vpx with a C-terminal FLAG tag, the *gag* gene of pSG-Gag cFLAG (Anraku *et al.*, 2010) was swapped with the *vpx* gene of pEF-Fvpx, and both the *vpx*-cFLAG portion and Kozak consensus sequence at the 5′ untranslated region were inserted into pEF1/*myc*-HisA (Life Technologies). The resultant plasmid was designated pEF-vpxF and used for expression of HIV-2 Vpx with a C-terminal FLAG tag. Various mutant clones were constructed from pEF-vpxF by PCR-based mutagenesis. An expression plasmid for SIVmac Vpx with an N-terminal FLAG tag was constructed by replacement of the *vpx* gene in pEF-Fvpx with SIVmac *vpx* gene (MA239 clone) (Shibata *et al.*, 1991), and designated pEF-Fvpx-SIVmac. Expression plasmids for an SIVmac Vpx mutant and HIV-2/SIVmac Vpx chimeras were generated by PCR-based mutagenesis using pEF-Fvpx and pEF-Fvpx-SIVmac. For *in vitro* transcription/translation analysis by *E. coli* S30 lysates, each *vpx* gene was inserted into pET-21b(+) (Novagen) to express Vpx with a FLAG tag at the N terminus (designated pET-Fvpx, pET-Fx106/4A, and pET-FxSt).

Transfection. Human 293T cells (Lebkowski *et al.*, 1985) were maintained in MEM medium containing 10 % heat-inactivated FBS and used for transfection experiments. For transfection, 2.5 μg of each expression plasmid DNA was introduced into 293T cells by the calcium-phosphate coprecipitation method (Adachi *et al.*, 1986). Cells were harvested at 24 h post-transfection for Western blot and RT-PCR analyses.

Western blotting. Western blot analysis was performed as described previously (Fujita *et al.*, 2008a, b). Cells were lysed in buffer composed of 10 mM Tris/HCl (pH 7.5), 10 mM NaCl, 1 % NP-40 and 1 % protease inhibitor cocktail (Sigma). Lysates were centrifuged for 5 min at 12 000 r.p.m. at 4 °C and the supernatants were used as samples after normalization of total protein amounts by a DC protein assay (Bio-Rad). Samples were separated on 12.5 or 15 % SDS-PAGE and transferred onto PVDF membranes (Immobilon-P; Millipore). The membranes were probed with anti-FLAG M2 antibody (Sigma) or anti-β-actin AC-15 antibody (Sigma), and with HRP-conjugated secondary antibody. Immunoreactive proteins were visualized by chemiluminescence using ECL Plus Western blotting detection reagents (GE Healthcare Bio-Sciences). Experiments were repeated at least three times, and the representative results are shown.

***In vitro* RNA transcription.** *In vitro* transcription was conducted by T7 RNA polymerase (New England Biolabs) using linearized plasmid DNAs (cut with *Xba*I) as templates. Transcribed RNA was quenched by EDTA and denatured by incubating at 65 °C for 15 min in MOPS, 50 % formamide and 12 % formaldehyde as indicated in the manufacturer's instructions. Denatured RNA was then mixed with ethidium bromide, separated by 1.5 % agarose gel containing MOPS and 18 % formaldehyde, and visualized by ethidium bromide staining. Experiments were repeated three times, and the representative results are shown.

***In vitro* transcription/translation.** A TNT T7 Quick Coupled Transcription/Translation System using rabbit reticulocyte lysates and a S30 T7 High-Yield Protein Expression System (Promega) were used to monitor the Vpx/Vpr expression in eukaryotic and prokaryotic cell-free systems, respectively. *In vitro* reactions were conducted according to the manufacturer's instructions. *In vitro* translated proteins were analysed by Western blotting. Experiments were repeated at least three times, and the representative results are shown.

Quantitative real-time RT-PCR. 293T cells were transfected with various expression plasmids, and harvested 24 h later. Levels of Vpx/Vpr mRNA in transfected cells were determined by quantitative real-time RT-PCR. After washes with PBS, total RNA was extracted with an RNeasy Plus Mini kit (Qiagen), and cDNA was synthesized using SuperScript III (Invitrogen) using oligo(dT) as a primer. PCR was performed with an ABI7500 (Applied Biosystems) using Power SYBR Green PCR Master Mix (Applied Biosystems). Primer sets used were: 5′-GCCAGGAAACAGTGGAGA-3′ and 5′-GCTTGGTGACATCCC-TTGGT-3′ for measurement of WT and mutant Vpx mRNAs; 5′-CTAGAGGGCCCTTCGAACAA-3′ and 5′-GCTGGCAACTAGAAG-GCACA-3′ for simultaneous measurement of Vpx and Vpr mRNAs. For normalization, a primer set specific for the human *GAPDH* gene (5′-CACCACCATGGAGAAGGCTG-3′ and 5′-GCTGATGATCTTG-AGGCTGTTGT-3′) was used. Values were calculated by the manufacturer's software. Standard curves were generated by amplifications of serially diluted cDNA samples. Experiments were repeated three times, and the mean values with standard deviations are presented.

Phylogenetic analysis. Phylogenetic analysis was performed for Vpx proteins of HIV-2/SIVs and Vpr proteins of the SIVagm group. PPM-minus SIVsyk Vpr was used as a reference. These amino acid sequences were obtained from the HIV sequence database at Los Alamos National Laboratory (http://www.hiv.lanl.gov) and aligned by the CLUSTAL_X 2.0.11 program (Jeanmougin *et al.*, 1998; Thompson *et al.*, 1997). Phylogenetic tree was generated by the neighbour-joining method using the CLUSTAL_X 2.0.11 program. The branch significance was analysed by bootstrap with 1000 replicates. The tree was visualized by the TreeView 1.6.6 program (Page, 1996) and the reference was manually removed.

ACKNOWLEDGEMENTS

We thank Ms Kazuko Yoshida for editorial assistance. This work was supported in part by the Japan Society for the Promotion of Science via a Grant-in-Aid for Young Scientists (B) to Y. M. (ID no. 24790443).

REFERENCES

Accola, M. A., Bukovsky, A. A., Jones, M. S. & Göttlinger, H. G. (1999). A conserved dileucine-containing motif in p6(gag) governs the particle association of Vpx and Vpr of simian immunodeficiency viruses SIV(mac) and SIV(agm). *J Virol* **73**, 9992–9999.

Adachi, A., Gendelman, H. E., Koenig, S., Folks, T., Willey, R., Rabson, A. & Martin, M. A. (1986). Production of acquired immunodeficiency syndrome-associated retrovirus in human and nonhuman cells transfected with an infectious molecular clone. *J Virol* **59**, 284–291.

Anraku, K., Fukuda, R., Takamune, N., Misumi, S., Okamoto, Y., Otsuka, M. & Fujita, M. (2010). Highly sensitive analysis of the interaction between HIV-1 Gag and phosphoinositide derivatives based on surface plasmon resonance. *Biochemistry* **49**, 5109–5116.

Berger, G., Durand, S., Fargier, G., Nguyen, X.-N., Cordeil, S., Bouaziz, S., Muriaux, D., Darlix, J.-L. & Cimarelli, A. (2011). APOBEC3A is a specific inhibitor of the early phases of HIV-1 infection in myeloid cells. *PLoS Pathog* **7**, e1002221.

Blanco-Melo, D., Venkatesh, S. & Bieniasz, P. D. (2012). Intrinsic cellular defenses against human immunodeficiency viruses. *Immunity* **37**, 399–411.

Doerfel, L. K., Wohlgemuth, I., Kothe, C., Peske, F., Urlaub, H. & Rodnina, M. V. (2013). EF-P is essential for rapid synthesis of proteins containing consecutive proline residues. *Science* **339**, 85–88.

Fujita, M., Otsuka, M., Miyoshi, M., Khamsri, B., Nomaguchi, M. & Adachi, A. (2008a). Vpx is critical for reverse transcription of the human immunodeficiency virus type 2 genome in macrophages. *J Virol* **82**, 7752–7756.

Fujita, M., Otsuka, M., Nomaguchi, M. & Adachi, A. (2008b). Functional region mapping of HIV-2 Vpx protein. *Microbes Infect* **10**, 1387–1392.

Fujita, M., Otsuka, M., Nomaguchi, M. & Adachi, A. (2010). Multifaceted activity of HIV Vpr/Vpx proteins: the current view of their virological functions. *Rev Med Virol* **20**, 68–76.

Goujon, C., Arfi, V., Pertel, T., Luban, J., Lienard, J., Rigal, D., Darlix, J.-L. & Cimarelli, A. (2008). Characterization of simian immunodeficiency virus SIV_{SM}/human immunodeficiency virus type 2 Vpx function in human myeloid cells. *J Virol* **82**, 12335–12345.

Gramberg, T., Sunseri, N. & Landau, N. R. (2010). Evidence for an activation domain at the amino terminus of simian immunodeficiency virus Vpx. *J Virol* **84**, 1387–1396.

Gutierrez, E., Shin, B.-S., Woolstenhulme, C. J., Kim, J.-R., Saini, P., Buskirk, A. R. & Dever, T. E. (2013). eIF5A promotes translation of polyproline motifs. *Mol Cell* **51**, 35–45.

Harris, R. S., Hultquist, J. F. & Evans, D. T. (2012). The restriction factors of human immunodeficiency virus. *J Biol Chem* **287**, 40875–40883.

Hrecka, K., Hao, C., Gierszewska, M., Swanson, S. K., Kesik-Brodacka, M., Srivastava, S., Florens, L., Washburn, M. P. & Skowronski, J. (2011). Vpx relieves inhibition of HIV-1 infection of macrophages mediated by the SAMHD1 protein. *Nature* **474**, 658–661.

Jeanmougin, F., Thompson, J. D., Gouy, M., Higgins, D. G. & Gibson, T. J. (1998). Multiple sequence alignment with CLUSTAL_X. *Trends Biochem Sci* **23**, 403–405.

Jin, L., Zhou, Y. & Ratner, L. (2001). HIV type 2 Vpx interaction with Gag and incorporation into virus-like particles. *AIDS Res Hum Retroviruses* **17**, 105–111.

Kawamura, M., Sakai, H. & Adachi, A. (1994). Human immunodeficiency virus Vpx is required for the early phase of replication in peripheral blood mononuclear cells. *Microbiol Immunol* **38**, 871–878.

Khamsri, B., Murao, F., Yoshida, A., Sakurai, A., Uchiyama, T., Shirai, H., Matsuo, Y., Fujita, M. & Adachi, A. (2006). Comparative study on the structure and cytopathogenic activity of HIV Vpr/Vpx proteins. *Microbes Infect* **8**, 10–15.

Laguette, N., Sobhian, B., Casartelli, N., Ringeard, M., Chable-Bessia, C., Ségéral, E., Yatim, A., Emiliani, S., Schwartz, O. & Benkirane, M. (2011). SAMHD1 is the dendritic- and myeloid-cell-specific HIV-1 restriction factor counteracted by Vpx. *Nature* **474**, 654–657.

Lebkowski, J. S., Clancy, S. & Calos, M. P. (1985). Simian virus 40 replication in adenovirus-transformed human cells antagonizes gene expression. *Nature* **317**, 169–171.

Mahnke, L. A., Belshan, M. & Ratner, L. (2006). Analysis of HIV-2 Vpx by modeling and insertional mutagenesis. *Virology* **348**, 165–174.

Malim, M. H. & Bieniasz, P. D. (2012). HIV restriction factors and mechanisms of evasion. *Cold Spring Harb Perspect Med* **2**, a006940.

Page, R. D. (1996). TreeView: an application to display phylogenetic trees on personal computers. *Comput Appl Biosci* **12**, 357–358.

Pancio, H. A. & Ratner, L. (1998). Human immunodeficiency virus type 2 Vpx-Gag interaction. *J Virol* **72**, 5271–5275.

Park, I.-W. & Sodroski, J. (1995). Amino acid sequence requirements for the incorporation of the Vpx protein of simian immunodeficiency virus into virion particles. *J Acquir Immune Defic Syndr Hum Retrovirol* **10**, 506–510.

Sharp, P. M., Bailes, E., Stevenson, M., Emerman, M. & Hahn, B. H. (1996). Gene acquisition in HIV and SIV. *Nature* **383**, 586–587.

Shibata, R., Kawamura, M., Sakai, H., Hayami, M., Ishimoto, A. & Adachi, A. (1991). Generation of a chimeric human and simian immunodeficiency virus infectious to monkey peripheral blood mononuclear cells. *J Virol* **65**, 3514–3520.

Singh, S. P., Lai, D., Cartas, M., Serio, D., Murali, R., Kalyanaraman, V. S. & Srinivasan, A. (2000). Epitope-tagging approach to determine the stoichiometry of the structural and nonstructural proteins in the virus particles: amount of Vpr in relation to Gag in HIV-1. *Virology* **268**, 364–371.

Thompson, J. D., Gibson, T. J., Plewniak, F., Jeanmougin, F. & Higgins, D. G. (1997). The CLUSTAL_X windows interface: flexible strategies for multiple sequence alignment aided by quality analysis tools. *Nucleic Acids Res* **25**, 4876–4882.

Ude, S., Lassak, J., Starosta, A. L., Kraxenberger, T., Wilson, D. N. & Jung, K. (2013). Translation elongation factor EF-P alleviates ribosome stalling at polyproline stretches. *Science* **339**, 82–85.

Ueno, F., Shiota, H., Miyaura, M., Yoshida, A., Sakurai, A., Tatsuki, J., Koyama, A. H., Akari, H., Adachi, A. & Fujita, M. (2003). Vpx and Vpr proteins of HIV-2 up-regulate the viral infectivity by a distinct mechanism in lymphocytic cells. *Microbes Infect* **5**, 387–395.

Zheng, Y.-H., Jeang, K.-T. & Tokunaga, K. (2012). Host restriction factors in retroviral infection: promises in virus-host interaction. *Retrovirology* **9**, 112.